Available online at www.sciencedirect.com
SCIENCE DIRECT®
Journal of Computational Physics 195 (2004) 434–464
JOURNAL OF COMPUTATIONAL PHYSICS
www.elsevier.com/locate/jcp

The Riemann problem for the Baer–Nunziato two-phase flow model

Nikolai Andrianov *, Gerald Warnecke

IAN, Otto-von-Guericke Universität Magdeburg, PSF 4120, D-39016 Magdeburg, Germany

Received 30 October 2002; received in revised form 29 September 2003; accepted 8 October 2003

Abstract

We consider the Riemann problem for the two-phase flow model, proposed by Baer and Nunziato [Int. J. Multiphase Flows 12 (1986) 861]. It describes the flame spread and the deflagration-to-detonation transition (DDT) in gas-permeable, reactive granular materials. The model is given by a non-strictly hyperbolic, non-conservative system of partial differential equations. We investigate the structure of the Riemann problem and construct the exact solution for it. We establish that the solution across one wave is not unique and propose to use the *evolutionarity criterion* to single out the admissible solution. Due to special structure of the Riemann problem for the Baer–Nunziato model, we are able to introduce a notion of a weak solution for it. Finally, we propose a number of test cases, based on the exact solution to the Riemann problem for the Baer–Nunziato model.

1. Introduction

One popular approach to describe two-phase flows is to use so-called *homogenized* or *averaged mixture models*. Within the framework of these models, the phases are treated as interpenetrating continua. The governing equations for the averaged phase quantities are obtained by averaging of the single-phase balance equations. For the derivation of such models, we refer to Ishii [17], Nigmatulin [22], Drew and Passman [10].

Homogenized models have been used to describe a large variety of two-phase flows. A partial list of references include spray modeling [8,25], deflagration-to-detonation transition (DDT) in gas-permeable, reactive granular materials [5,6,11,14,18,19,23], multiphase mixtures [26], and bubble flow [13].

Nowadays, a more or less established model is given by a system of partial differential equations, which includes the two continuity, two momentum, and two energy equations for both phases. The averaging of

* Corresponding author.
E-mail addresses: nikolai.andrianov@mathematik.uni-magdeburg.de (N. Andrianov), gerald.warnecke@mathematik.uni-magdeburg.de (G. Warnecke).

0021-9991/$ - see front matter © 2003 Elsevier Inc. All rights reserved.
doi:10.1016/j.jcp.2003.10.006

the single phase equations results in additional terms, which describe the interaction between the phases. These are the mass transfer terms for the continuity equations, the momentum exchange terms for the momentum equations, and the energy exchange terms for the energy equations. The exact expressions for the transfer terms are usually unknown and one has to use some additional considerations (experimental data, simplified models, etc.) to formulate them.

Mathematically, the phase interaction is described with both *differential* interaction terms, and *non-differential* source terms. Due to the differential interaction terms the overall system of governing equations cannot be written in divergence form. It is said that the system is *non-conservative*, in opposite to conservation laws, which by definition are in divergence form. The differential phase interaction terms, which prevent the system from being conservative, are called *non-conservative terms*.

The non-conservative character of the system has major consequences both for its mathematical analysis, and numerical solution. Concerning the mathematical analysis, one has the following issues. It is clear that the solution may become discontinuous, e.g., via a shock wave. Then, the differentiation is not determined in the classical sense, so one needs to introduce a *weak solution*. However, since the system is non-conservative, one cannot use the corresponding definition from the theory of distributions used for conservation laws. Also, one cannot define the Rankine–Hugoniot shock conditions as it is done for conservation laws.

Numerically, one has difficulties in discretizing the non-conservative terms. Currently, the theory of numerical methods for non-conservative systems is largely absent. There is no criterion how one should design a numerical scheme for such systems. Also, there is a lack of test problems with an exact solution. Therefore, it is difficult to compare different numerical methods for non-conservative systems.

This paper is concerned with the study of one of the most established non-conservative models for two-phase flows, the Baer–Nunziato (BN) model [5]. It describes the deflagration-to-detonation transition (DDT) in gas-permeable, reactive granular materials. We restrict ourselves to the *homogeneous* BN model, i.e., without the non-differential phase interaction terms, and investigate a simple initial-value problem for it, the *Riemann problem*. Our interest in this problem is motivated by its relatively simple mathematical structure, compared to the models for multiphase mixtures [26] or two-phase flows with micro-inertia [13]. We believe that the investigation of the homogeneous BN model can give a guideline in the study of more complicated models like those mentioned above. Also, a solution to the Riemann problem provides a building block for a wide class of numerical methods, namely the Godunov-type methods, see e.g. [29] for a review. Finally, the exact solution to the Riemann problem is an invaluable test case which is useful in assessing the performance of numerical methods.

The main results of the paper are the following. We present a procedure to construct exact solutions to the Riemann problem for the homogeneous BN model. The usual ''direct'' solution to this problem consists in finding a solution for given initial data. However, this appears to be very complicated: The waves in the solution can overlap with each other, so one has to consider a number of different cases. Instead, we propose what we call the ''inverse'' solution to the Riemann problem: We *fix* the configuration of the Riemann problem, and look for initial data which are compatible with it. We note that the solution to the Riemann problem for the homogeneous BN model is *not unique*. This follows from our work [4].

It appears that the solution across one wave, the solid contact discontinuity, is also not unique: For a given state on one side of it, there exist up to two possible states on the other side. We propose a selection criterion for the admissible solution: The *evolutionarity criterion*. The notion of evolutionarity is discussed in the context of gas dynamics, see e.g. [20, § 87], and in magnetohydrodynamics, see e.g. [12].

Finally, we propose a number of test cases for the homogeneous BN model, using the ''inverse'' solution to the Riemann problem described above. Note that the mathematical structure of the BN model is similar to the structure of several other models [13,26]. Therefore, one can try numerical methods for the non-conservative models of the type [13,26] on the test cases for the homogeneous BN model, and compare the numerical results with the exact solution.

The paper is organized as follows. In Section 2, we briefly present the characteristic analysis of the homogeneous BN model. Section 3 is devoted to investigating the properties of the solid contact discontinuity in the solution to the Riemann problem. In Section 4, we study the analogies between the flow inside of the solid contact and the classical converging–diverging nozzle, see e.g. [7, Chapter V]. In Section 5, we note that for the Riemann problem, the original *non-conservative* system of governing equations is equivalent to some *conservative* system locally. This allows us to introduce the notion of a weak solution for the Riemann problem. In Section 6, we describe the procedure of the "inverse" solution to the Riemann problem for the homogeneous BN model. Section 8 is devoted to the cases when some of the waves in the solution of the Riemann problem approach each other and coincide in the limit. Finally, in Section 9, we propose several test problems, based on the exact solution of the Riemann problem. As an example, we assess the performance of the method for compressible multiphase flows which we have proposed in [3], and discuss the results.

2. Characteristic analysis

The characteristic analysis of the BN model was carried out by Embid and Baer [11]. Therefore, here we will only present the results which are used in subsequent sections; for details we refer to [11].

Since the BN model [5] describes the flame spread in gas-permeable granular solids, the two phases under consideration are *solid* and *gas*. We will denote them with subscripts a and b, respectively. Let ρ_k be the density, u_k the velocity, p_k the pressure, E_k the total specific energy, and α_k the volume fraction of the phase $k = \mathrm{a}, \mathrm{b}$. Then, the system of governing equations for the homogeneous BN model can be written in the following form:

$$\frac{\partial \mathbf{u}}{\partial t} + \frac{\partial \mathbf{f}(\mathbf{u})}{\partial x} = \mathbf{h}(\mathbf{u}) \frac{\partial a_{\mathrm{a}}}{\partial x}, \tag{2.1}$$

with

$$\mathbf{u} = \begin{bmatrix} \alpha_{\mathrm{a}} \\ \alpha_{\mathrm{a}}\rho_{\mathrm{a}} \\ \alpha_{\mathrm{a}}\rho_{\mathrm{a}}u_{\mathrm{a}} \\ \alpha_{\mathrm{a}}\rho_{\mathrm{a}}E_{\mathrm{a}} \\ \alpha_{\mathrm{b}}\rho_{\mathrm{b}} \\ \alpha_{\mathrm{b}}\rho_{\mathrm{b}}u_{\mathrm{b}} \\ \alpha_{\mathrm{b}}\rho_{\mathrm{b}}E_{\mathrm{b}} \end{bmatrix}, \quad \mathbf{f}(\mathbf{u}) = \begin{bmatrix} 0 \\ \alpha_{\mathrm{a}}\rho_{\mathrm{a}}u_{\mathrm{a}} \\ \alpha_{\mathrm{a}}\rho_{\mathrm{a}}u_{\mathrm{a}}^2 + \alpha_{\mathrm{a}}p_{\mathrm{a}} \\ \alpha_{\mathrm{a}}u_{\mathrm{a}}(\rho_{\mathrm{a}}E_{\mathrm{a}} + p_{\mathrm{a}}) \\ \alpha_{\mathrm{b}}\rho_{\mathrm{b}}u_{\mathrm{b}} \\ \alpha_{\mathrm{b}}\rho_{\mathrm{b}}u_{\mathrm{b}}^2 + \alpha_{\mathrm{b}}p_{\mathrm{b}} \\ \alpha_{\mathrm{b}}u_{\mathrm{b}}(\rho_{\mathrm{b}}E_{\mathrm{b}} + p_{\mathrm{b}}) \end{bmatrix}, \quad \mathbf{h}(\mathbf{u}) = \begin{bmatrix} -u_{\mathrm{a}} \\ 0 \\ +p_{\mathrm{b}} \\ +p_{\mathrm{b}}u_{\mathrm{a}} \\ 0 \\ -p_{\mathrm{b}} \\ -p_{\mathrm{b}}u_{\mathrm{a}} \end{bmatrix}. \tag{2.2}$$

In what follows, we will consider the Riemann problem for the system (2.1), i.e., equip it with piecewise constant initial data

$$\mathbf{u}(x,0) = \begin{cases} \mathbf{u}_{\mathrm{L}}, & x \leqslant 0, \\ \mathbf{u}_{\mathrm{R}}, & x > 0. \end{cases} \tag{2.3}$$

As usual, we will assume that the solution to the Riemann problem (2.1) and (2.3) is self-similar, i.e.,

$$\mathbf{u}(x,t) = \mathbf{u}(\xi), \quad \xi = \frac{x}{t}.$$

Observe that the system (2.1) cannot be written in divergence form, i.e., it is *non-conservative*. Indeed, the non-conservative terms $\mathbf{h}(\mathbf{u})(\partial\alpha_{\mathrm{a}}/\partial x)$ and the first equation of (2.1) prevent it from being written in divergence form. Note that for the case $\alpha_{\mathrm{a}} = \text{const.}$, the system decouples into the two sets of Euler equations

for the phases a and b. For the mixture, one can get the *conservative* balance equations by summing the corresponding single-phase equations.

It is clear that the solution to (2.1) can become discontinuous, e.g., across a shock wave. Then, the differentiation in (2.1) is not determined in the classical sense and one needs to define a weak solution for (2.1). However, it is not possible to do this analogously to conservation laws, as in, e.g. [28]. Also, it is not clear what are the Rankine–Hugoniot shock relations for (2.1) in case of $\alpha_a \neq \text{const}$. A definition of a weak solution for general non-conservative systems was given by Dal Maso et al. [9]. In Section 5, we give a different definition of a weak solution for the particular case of the Riemann problem (2.1) and (2.3). We can also easily obtain the Rankine–Hugoniot shock relations for the Riemann problem to (2.1) and (2.3), see Sections 5 and 8.2.

In order to close the system (2.1), we need to provide additional relations. One of these relations is the saturation constraint

$$\alpha_a + \alpha_b = 1.$$

Two further relations are the equations of state (EOS) for each phase. In order to avoid difficulties with thermodynamic modeling of solid materials, we use the so-called stiffened gas EOS [21] for each phase,

$$e_k = \frac{p_k + \gamma_k \pi_k}{\rho_k(\gamma_k - 1)}, \quad k = a, b, \tag{2.4}$$

where γ_k and π_k are the constants, specific for the phase k. One can show that this EOS satisfies the standard convexity assumptions of gas dynamics [7].

For simplicity, let us rewrite the system (2.1) in primitive variables

$$\frac{\partial \mathbf{v}}{\partial t} + \mathbf{A}(\mathbf{v})\frac{\partial \mathbf{v}}{\partial x} = 0, \tag{2.5}$$

with

$$\mathbf{A} = \begin{bmatrix} u_a & 0 & 0 & 0 & 0 & 0 & 0 \\ 0 & u_a & \rho_a & 0 & 0 & 0 & 0 \\ \frac{p_a - p_b}{\alpha_a \rho_a} & 0 & u_a & 1/\rho_a & 0 & 0 & 0 \\ 0 & 0 & \rho_a c_a^2 & u_a & 0 & 0 & 0 \\ -\frac{\rho_b}{\alpha_b}(u_b - u_a) & 0 & 0 & 0 & u_b & \rho_b & 0 \\ 0 & 0 & 0 & 0 & 0 & u_b & 1/\rho_b \\ -\frac{\rho_b c_b^2}{\alpha_b}(u_b - u_a) & 0 & 0 & 0 & 0 & \rho_b c_b^2 & u_b \end{bmatrix}, \quad \mathbf{v} = \begin{bmatrix} \alpha_a \\ \rho_a \\ u_a \\ p_a \\ \rho_b \\ u_b \\ p_b \end{bmatrix}. \tag{2.6}$$

The eigenvalues of the matrix $\mathbf{A}(\mathbf{v})$ are

$$\begin{aligned} &\lambda_0 = u_a, \\ &\lambda_1 = u_a - c_a, \quad \lambda_2 = u_a, \quad \lambda_3 = u_a + c_a, \\ &\lambda_4 = u_b - c_b, \quad \lambda_5 = u_b, \quad \lambda_6 = u_b + c_b, \end{aligned} \tag{2.7}$$

where $c_k = \sqrt{\gamma_k(p_k + \pi_k)/\rho_k}$ is the sound speed, $k = a, b$. Since all of the eigenvalues (2.7) are real, the system (2.1) is hyperbolic, although not strictly hyperbolic. Indeed, situations are possible, when some of the eigenvalues of the solid phase can coincide with some of the gas phase. Note also that $\lambda_0 = \lambda_2 = u_a$ is a double eigenvalue.

In [11], it was shown that the eigenvectors of the matrix $\mathbf{A}(\mathbf{v})$ become linearly dependent in the points in the flow, where any one of conditions

$$\alpha_a = 0, \quad \alpha_b = 0, \quad c_b^2 - (u_b - u_a)^2 = 0 \tag{2.8}$$

holds. In this case, the system (2.1) is said to be *parabolic degenerate*, i.e., not hyperbolic anymore. In what follows, we will always consider two-phase *mixtures*, i.e., the case of pure phases $\alpha_a = 0$ and $\alpha_b = 0$ will be excluded. In Section 8.3, we provide a physical interpretation for the degenerate case $c_b^2 - (u_b - u_a)^2 = 0$.

The analysis of [11] shows that the 1-, 3-, 4-, and 6-characteristic fields are genuinely nonlinear, and the 0-, 2-, and 5-fields are linearly degenerate. There are six Riemann invariants for the 1-, 2-, and 3-characteristic fields, namely,

- Two invariants, analogous to the ones for single-phase gas dynamics, see e.g. [29].
- Three invariants, expressing the constancy of gas variables, e.g., ρ_b, u_b, p_b.
- The solid volume fraction α_a.

There are six Riemann invariants for the 4-, 5-, and 6-characteristic fields, namely,

- Two invariants, analogous to the ones for single-phase gas dynamics.
- Three invariants, expressing the constancy of solid variables, e.g., ρ_a, u_a, p_a.
- The solid volume fraction α_a.

Finally, there are five Riemann invariants for the 0-characteristic field, since the eigenvalue $\lambda_0 = \lambda_2 = u_a$ has *constant* multiplicity equal to 2. They are

$$\begin{aligned}
\psi_1 &= u_a, \\
\psi_2 &= \eta_b, \\
\psi_3 &= \alpha_b \rho_b (u_a - u_b), \\
\psi_4 &= \alpha_a p_a + \alpha_b p_b + \alpha_b \rho_b (u_a - u_b)^2, \\
\psi_5 &= \frac{(u_a - u_b)^2}{2} + \frac{c_b^2}{\gamma_b - 1},
\end{aligned} \tag{2.9}$$

where $\eta_b = (p_b + \pi_b)/\rho_b^{\gamma_b}$ is the isentrope of phase b.

The solution to the Riemann problem (2.1) and (2.3) is composed of shocks, rarefaction waves, and contact discontinuities. Across the rarefaction waves and contacts, the corresponding Riemann invariants are constant.

3. Properties of the solid contact

The solid contact discontinuity, which corresponds to the 0-characteristic field, plays a special role in the solution to the Riemann problem (2.1) and (2.3). As we have seen in Section 2, the volume fraction α_a changes only across this wave. Therefore, the non-conservative terms of the system (2.1), i.e., $\mathbf{h}(\mathbf{u})(\partial\alpha_a/\partial x)$ and the first equation of (2.1), act only along the solid contact. Consequently, the study of the solid contact will reveal the role of the non-conservative terms of the system (2.1). Here, we assume for simplicity that the solid contact does not coincide with other waves in the solution to the Riemann problem (2.1) and (2.3). The case of coinciding waves will be considered as a limit case in Section 8.

Denote the variables to the left of the solid contact by the subscript 0 and the variables to the right of it right by the subscript 1. Across the solid contact, the Riemann invariants (2.9) are constant,

$$u_{a0} = u_{a1} =: u_a, \tag{3.1a}$$

$$\eta_{b0} = \eta_{b1} =: \eta_b, \tag{3.1b}$$

$$\alpha_{b0}\rho_{b0}(u_{b0}-u_a)=\alpha_{b1}\rho_{b1}(u_{b1}-u_a)=:M, \tag{3.1c}$$

$$\alpha_{a0}p_{a0}+\alpha_{b0}p_{b0}+\alpha_{b0}\rho_{b0}(u_{b0}-u_a)^2=\alpha_{a1}p_{a1}+\alpha_{b1}p_{b1}+\alpha_{b1}\rho_{b1}(u_{b1}-u_a)^2=:P, \tag{3.1d}$$

$$\frac{(u_{b0}-u_a)^2}{2}+\frac{c_{b0}^2}{\gamma_b-1}=\frac{(u_{b1}-u_a)^2}{2}+\frac{c_{b1}^2}{\gamma_b-1}=:E. \tag{3.1e}$$

Observe that the solid density ρ_a does not appear in (3.1), it acts as a free parameter. Note also, that the system (3.1) is an *underdetermined* system for the parameters at the left and at the right of the solid contact. Indeed, we have 14 unknowns

$$\alpha_{ai},\ \rho_{ai},\ u_{ai},\ p_{ai},\ \rho_{bi},\ u_{bi},\ p_{bi},\quad i=0,1$$

but only five equations. Therefore, one has to fix nine unknowns. We choose to fix the following variables:

$$\alpha_{a0},\ \rho_{a0},\ u_{a0},\ p_{a0},\ \rho_{b0},\ u_{b0},\ p_{b0},\ \alpha_{a1},\ \rho_{a1}.$$

Then, the number of the equations in (3.1) and the number of unknowns coincide and one might hope to get a solution.

Note that the system (3.1) is reminiscent of the mass, momentum, and energy balance across a discontinuity, propagating with the speed u_a, for the Euler equations for the gas phase. Consider the case

$$\alpha_{b0}=\alpha_{b1},$$

and the other parameters keep their values. Remember that this corresponds to the decoupled Euler equations for the gas and solid phases, see the system (2.1). So, the gas flow does not see the solid phase, and obviously the gas parameters do not change across u_a. Thus, there always exists the trivial solution

$$\begin{aligned}&\rho_{b0}=\rho_{b1},\\&u_{b0}=u_{b1},\\&p_{b0}=p_{b1}.\end{aligned} \tag{3.2}$$

Note that this is the unique *admissible* solution of (3.1). In what follows, we will refer to this case as "Euler", and the case

$$\alpha_{b0}\neq\alpha_{b1}$$

as "multiphase". In what follows, we will often fix the phase variables ρ_k,u_k,p_k, $k=a,b$, and consider the Euler case $\alpha_{b0}=\alpha_{b1}$ and the multiphase case $\alpha_{b0}\neq\alpha_{b1}$. If we let

$$\frac{\alpha_{b0}}{\alpha_{b1}}\to 1,$$

then the multiphase case will turn into the Euler case.

Combining the equations of (3.1), we get the following nonlinear equation for the gas density to the right of u_a

$$F(\rho_{b1})=\frac{1}{2}\left(\frac{M}{\alpha_{b1}\rho_{b1}}\right)^2+\frac{\gamma_b\eta_b\rho_{b1}^{\gamma_b-1}}{\gamma_b-1}-E=0. \tag{3.3}$$

The derivative of $F(\rho)$ is

$$F'(\rho) = -\frac{M^2}{\alpha_{b1}^2 \rho^3} + \gamma_b \eta_b \rho^{\gamma_b - 2}. \tag{3.4}$$

At the point ρ_*, the function $F(\rho)$ reaches its minimum

$$\rho_* = \left(\frac{M^2}{\alpha_{b1}^2 \gamma_b \eta_b} \right)^{(1/(\gamma_b+1))}. \tag{3.5}$$

Indeed, for all $\rho < \rho_*$ we have

$$\rho^{\gamma_b+1} < \rho_*^{\gamma_b+1} = \frac{M^2}{\alpha_{b1}^2 \gamma_b \eta_b},$$

giving

$$\gamma_b \eta_b \rho^{\gamma_b - 2} < \frac{M^2}{\alpha_{b1}^2 \rho^3}.$$

Consequently,

$$F'(\rho) < 0$$

for all $\rho < \rho_*$. Analogously,

$$F'(\rho) > 0$$

for all $\rho > \rho_*$. Note also that $F(\rho) \to +\infty$ as $\rho \to +0$ or $\rho \to +\infty$.

Depending on the sign of $F(\rho_*)$, Eq. (3.3) can have no, one, or two roots. We will investigate each case separately.

3.1. No roots

Consider the solid particle speed invariants (3.1). We will fix the left state 0, and look for the root of Eq. (3.3) for the variable right gas volume fraction α_{b1}.

We can rewrite (3.1c) as

$$\rho_{b0}(u_{b0} - u_a) = \frac{\alpha_{b1}}{\alpha_{b0}} \rho_{b1}(u_{b1} - u_a) = \frac{M}{\alpha_{b0}} =: M_E,$$

where the subscript E stands for Euler. Indeed, M_E is equal to the mass flow for the Euler case $\alpha_{b0} = \alpha_{b1}$. With a *constant* α_{b0}, we have the constant M_E at the right-hand side.

Let us rewrite Eq. (3.3) as follows:

$$F(\rho_{b1}) = \frac{1}{2} M_E^2 \left(\frac{\alpha_{b0}}{\alpha_{b1}} \right)^2 \frac{1}{\rho_{b1}^2} + \frac{\gamma_b \eta_b \rho_{b1}^{\gamma_b - 1}}{\gamma_b - 1} - E = 0. \tag{3.6}$$

For the Euler case

$$\frac{\alpha_{b0}}{\alpha_{b1}} = 1$$

and (3.6) always has at least one trivial solution (3.2). For variable $\alpha_{b1} \in]0, 1[$ (multiphase case), we have

$$\frac{\alpha_{b0}}{\alpha_{b1}} \in]\alpha_{b0}, \infty[.$$

It is obvious that if for some positive C, C big enough,

$$\frac{\alpha_{b0}}{\alpha_{b1}} > C, \tag{3.7}$$

then (3.6) has no roots, since $E, \eta_b, \rho_b > 0$ and $\gamma_b > 1$. Thus for all α_{b1}, $\alpha_{b1} < \alpha_{b0}/C$, Eq. (3.6) has no roots. Decreasing α_{b1} (or increasing α_{a1}, $\alpha_{a1} = 1 - \alpha_{b1}$), one necessarily gets no solution for some value of α_{b1}.

3.2. One or two roots

Consider again the equations

$$F(\rho_{b1}) = \frac{1}{2}\left(\frac{M}{\alpha_{b1}\rho_{b1}}\right)^2 + \frac{\gamma_b \eta_b \rho_{b1}^{\gamma_b - 1}}{\gamma_b - 1} - E = 0 \tag{3.8}$$

$$F'(\rho) = -\frac{M^2}{\alpha_{b1}^2 \rho^3} + \gamma_b \eta_b \rho^{\gamma_b - 2}. \tag{3.9}$$

Suppose first that (3.8) has two roots. Denote them $\tilde{\rho}_{b1}$, $\tilde{\tilde{\rho}}_{b1}$,

$$\tilde{\rho}_{b1} < \tilde{\tilde{\rho}}_{b1},$$

see Fig. 1. Then

$$F'(\tilde{\rho}_{b1}) < 0, \quad F'(\tilde{\tilde{\rho}}_{b1}) > 0.$$

Using (3.1c)

$$\frac{M^2}{\alpha_{b1}^2} = (u_{b1} - u_a)^2 \rho_{b1}^2$$

we can rewrite (3.9) as

$$-(u_{b1} - u_a)^2 + c_{b1}^2 = F'(\rho_{b1})\rho_{b1}, \tag{3.10}$$

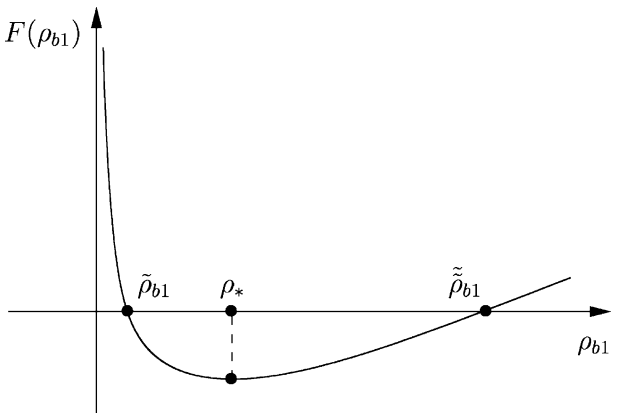

Fig. 1. Graph of $F(\rho_{b1})$.

where $c_{b1}^2 = \gamma_b(p_{b1} + \pi_b)/\rho_{b1}$ is the gas sound speed squared. We see that the volume fraction α_b does not appear in this equation. This means that it should hold for any values of α_{b0}, α_{b1} on both sides of the soild contact. In particular, for the Euler case $\alpha_{b0} = \alpha_{b1}$, the admissible solution is (3.2),

$$\rho_{b0} = \rho_{b1},$$
$$u_{b0} = u_{b1},$$
$$p_{b0} = p_{b1}.$$

Thus, we have the two roots $\tilde{\rho}_{b1}, \tilde{\tilde{\rho}}_{b1}$ of (3.8) as candidates for ρ_{b1}. We choose the one for which

$$\operatorname{sign}(-(u_{b0} - u_a)^2 + c_{b0}^2) = \operatorname{sign}(-(u_{b1} - u_a)^2 + c_{b1}^2) \tag{3.11}$$

since all these quantities are identical on the left- and right-hand side. By (3.10), it is equivalent to the condition

$$\operatorname{sign}(F'(\rho_{b0})) = \operatorname{sign}(F'(\rho_{b1})). \tag{3.12}$$

For the multiphase case $\alpha_{b0} \neq \alpha_{b1}$, we also choose by a continuity argument the root of (3.8), which satisfies the condition (3.12). It corresponds to the admissible root for the Euler case, if α_{b1} would be equal to α_{b0}.

A motivation for this choice is the following. Consider the Euler case $\alpha_{b0} = \alpha_{b1}$, and let the admissible Euler root be $\tilde{\rho}_{b1}$. Then, it satisfies the criterion (3.12). Now let us deviate the ratio α_{b0}/α_{b1} slightly, i.e,

$$\frac{\alpha_{b0}}{\alpha_{b1}} := 1 + \epsilon, \quad \epsilon \text{ small}.$$

Then, for this *multiphase* case the admissible root is also $\tilde{\rho}_{b1}$, it cannot suddenly become $\tilde{\tilde{\rho}}_{b1}$. We summarize these ideas by formulating the following definition.

Definition 3.1. The physically admissible state behind the solid contact is determined by the root of (3.3), which satisfies the condition (3.11).

The case of the single root of (3.8) corresponds to the degenerate situation, when the gas velocity relative to u_a is sonic to the right of Σ, i.e., $|u_{b1} - u_a| = c_{b1}$. We will discuss this case in greater detail in Section 8.3.

3.3. Evolutionary discontinuities

The above results show that the solution across the solid contact is not unique. That is, for a fixed state on one side of it, one can find at most two states on the other side of it. Then, one of these states is considered to be non-admissible according to Definition 3.1. Note that the condition behind it is actually more intuitive than physical. Also, it is restricted only to the Riemann problem for the BN model.

However, a non-unique solution across a discontinuity is not something reserved for a particular system. It is well known that for a *general* conservation law, a weak solution is not unique, see, e.g. [28]. In that case, one employs different kinds of *entropy conditions*, in order to rule out the non-physical solutions.

A naive use of an entropy condition would be to look at the entropy across the solid contact and to draw conclusions on its basis. Observe that this would not work: Entropy is constant across the solid contact, see (3.1b). We also cannot use the entropy inequality from the theory of conservation laws, see, e.g. [28], since the system (2.1) is non-conservative.

In order to single out one solution across the solid contact, we propose to use the following admissibility criterion.

Definition 3.2 (*Evolutionarity criterion*). Consider a discontinuity Σ in a physical flow, which is governed by a $p \times p$ hyperbolic system. Denote the number of characteristics, incoming to Σ by n and coinciding with Σ by c. Further, denote the number of unknown variables on the both sides of Σ together with its speed by $N = 2p + 1$ and the number of relations across Σ by m. Then Σ is called evolutionary, if

$$N = n + c + m.$$

For the evolutionary discontinuity Σ, all N variables on it can be found using $n + c$ relations along the incoming and coinciding characteristics, and m relations across Σ. Therefore, Σ is well determined in the flow, i.e., it *evolves* in time.

The notion of *evolutionarity* goes back to at least Landau and Lifshitz [20, § 87], who studied the stability of shock waves in gas dynamics. Evolutionary discontinuities are also discussed in context of magnetohydrodynamics, see e.g. [12].

In order for a contact discontinuity to be evolutionary, the number of characteristics impinging on it from the one side must be equal to the number of characteristics leaving it from the other side.

For a strictly hyperbolic system, the evolutionarity criterion is equivalent to the Lax shock condition. For *resonant* hyperbolic systems, i.e., for systems of type (4.2), it is equivalent to the criterion of Isaacson and Temple [15,16]. For proofs of the above statements, see [2].

3.4. Evolutionarity of the solid contact

Let us investigate, under which conditions the solid contact Σ will be an evolutionary discontinuity. For simplicity, we assume that there are no gas characteristics which coincide with Σ. The case of coinciding gas characteristics will be considered in Section 8.

Denote the number of characteristics, impinging on the solid contact Σ from the both sides by n, coinciding with Σ by c, and leaving it by s. Since the order of the system (2.1) is $p = 7$, there will be $N = 2p + 1 = 15$ unknowns at Σ. Across the solid contact Σ, the $p - 2 = 5$ Riemann invariants are constant. Since the speed of Σ is $u_a = \lambda_0 = \lambda_2$, there are $m = 5 + 1 = 6$ conditions across it. Also, there are $c = 2 + 2 = 4$ solid characteristics, coinciding with Σ from the both sides.

According to Definition 3.2, the solid contact will be evolutionary if

$$N = n + c + m.$$

Using the values for N, c, and m found above, we obtain

$$15 = n + 4 + 6, \quad \text{so } n = 5. \tag{3.13}$$

At this stage, it is advantageous to separate the incoming characteristics according to the phases a and b. Denote the number of the incoming characteristics for the solid phase by n_a and for the gas phase by n_b, so that $n = n_a + n_b$. Remember that the characteristics of each phase are *ordered*, cf. (2.7). Since the characteristics with the speed $\lambda_0 = \lambda_2 = u_a$ coincide with the solid contact Σ, the characteristic with the speed $\lambda_3(\mathbf{u}_0) = u_{a0} + c_{a0}$ will always impinge on Σ from the left, and the one with $\lambda_1(\mathbf{u}_1) = u_{a1} - c_{a1}$ from the right. Therefore, we have

$$n_a = 2.$$

Using this in (3.13), we obtain

$$n_b = 3. \tag{3.14}$$

We have thus proved the following theorem.

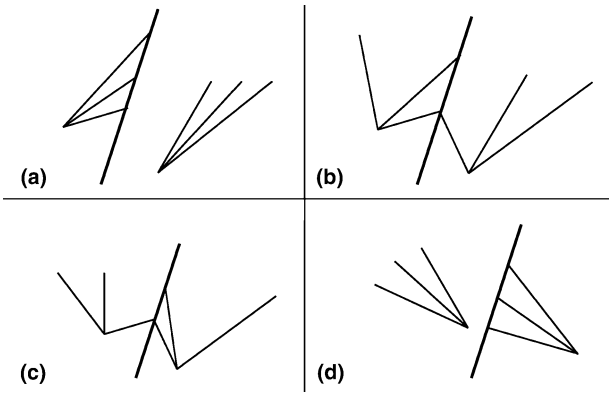

Fig. 2. Four possible positions of the gas characteristics around an evolutionary solid contact.

Theorem 3.3. *Consider the Riemann problem* (2.1) *and* (2.3) *and assume that there are no gas characteristics, which coincide with the solid contact* Σ*, propagating with the velocity* u_a*. Then* Σ *is evolutionary iff there are precisely three gas characteristics, which impinge on it from the both sides.*

Next, let us show that if the state behind the solid contact is physically admissible in the sense of Definition 3.1, then the solid contact is an evolutionary discontinuity.

Theorem 3.4. *Consider the Riemann problem* (2.1) *and* (2.3) *and assume that there are no gas characteristics, which coincide with the solid contact* Σ*, propagating with the velocity* u_a*. Then* Σ *is evolutionary iff the state behind* Σ *is physically admissible in the sense of Definition* 3.1 *i.e.*,

$$\operatorname{sign}(-(u_{b0}-u_a)^2+c_{b0}^2)=\operatorname{sign}(-(u_{b1}-u_a)^2+c_{b1}^2). \tag{3.15}$$

Proof. From the constancy of the third Riemann invariant across the solid contact, i.e., from (3.1c), it follows that

$$u_{b0}<u_a \iff u_{b1}<u_a.$$

Analogously,

$$u_{b0}>u_a \iff u_{b1}>u_a.$$

Considering different cases in Eq. (3.15), we can find different positions of the gas characteristics around the evolutionary solid contact, see Fig. 2. In each case in Fig. 2, there are precisely three gas characteristics, which impinge on the solid contact. By Theorem 3.3, the solid contact Σ is then an evolutionary discontinuity. □

4. Gas dynamics analogy

It has been recognized by several authors [6,11,27] that the homogeneous BN model (2.1) is reminiscent of the Euler equations in the duct of variable cross-section $A=A(x)$,

$$\begin{aligned}
&\frac{\partial A\rho}{\partial t}+\frac{\partial A\rho v}{\partial x}=0,\\
&\frac{\partial A\rho v}{\partial t}+\frac{\partial A(\rho v^2+p)}{\partial x}=p\frac{\partial A}{\partial x},\\
&\frac{\partial A\rho E}{\partial t}+\frac{\partial Av(\rho E+p)}{\partial x}=0.
\end{aligned}\tag{4.1}$$

For a derivation, we refer to, e.g. [30]. Usually, the cross-section $A = A(x)$ is assumed to be a priori given. However, we can consider it as an additional unknown, and supply the trivial equation $A_t = 0$ for determining it. Then, the system (4.1) becomes

$$\begin{aligned}
&\frac{\partial A}{\partial t}=0,\\
&\frac{\partial A\rho}{\partial t}+\frac{\partial A\rho v}{\partial x}=0,\\
&\frac{\partial A\rho v}{\partial t}+\frac{\partial A(\rho v^2+p)}{\partial x}=p\frac{\partial A}{\partial x},\\
&\frac{\partial A\rho E}{\partial t}+\frac{\partial Av(\rho E+p)}{\partial x}=0.
\end{aligned}\tag{4.2}$$

We can close this system with the stiffened gas EOS,

$$e=\frac{p+\gamma\pi}{\rho(\gamma-1)},$$

where γ and π are thermodynamic constants.

Note that the system (4.2) can be formally obtained from the homogeneous BN model (2.1), if one sets there

$$u_{\mathrm{a}} := 0 \tag{4.3}$$

and uses the correspondence

$$(\alpha_{\mathrm{b}}, \rho_{\mathrm{b}}, u_{\mathrm{b}}, p_{\mathrm{b}}, E_{\mathrm{b}}) \leftrightarrow (A, \rho, v, p, E). \tag{4.4}$$

Thus, the volume fraction of the phase b plays the role of the variable cross-section A, and the density, velocity, pressure, and energy of the phase b have the corresponding meanings for the gas flow in a duct of variable cross-section.

The stationary smooth solutions of the system (4.2) are given by

$$\begin{aligned}
&A\rho v=\text{const.},\\
&\eta=\text{const.},\\
&\frac{v^2}{2}+\frac{c^2}{\gamma-1}=\text{const.},
\end{aligned}\tag{4.5}$$

where $\eta = (p+\pi)/\rho^{\gamma}$ is the isentrope and $c=\sqrt{\gamma(p+\pi)/\rho}$ is the sound speed, see e.g. [7]. These relations express the conservation of mass, entropy, and Bernoulli's law, respectively.

Note that the relations (4.5) are very much similar to Eqs. (3.1), expressing the constancy of the Riemann invariants across the solid contact. This gives us the reason to consider the solid contact as the porous film of the infinitesimal thickness δ, see Fig. 3. Each pore represents a duct of variable cross-section. The solid phase forms the walls of the duct. The values of α_{b} at the both sides of this porous film are given and equal

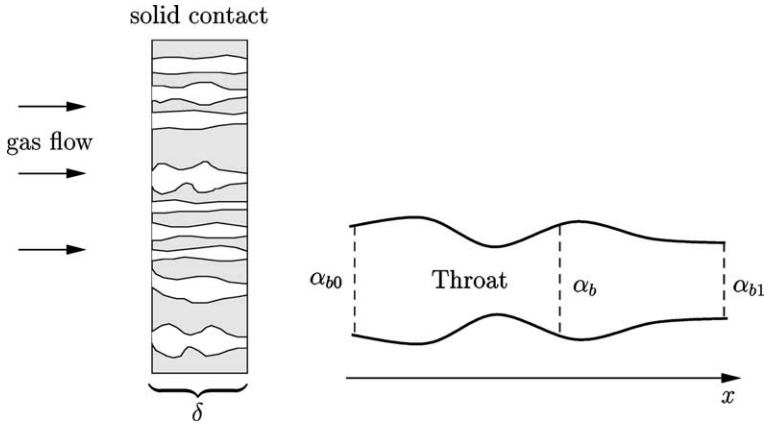

Fig. 3. Left: Gas flow through the solid contact. Right: a pore of the variable cross-section.

to α_{b0} and α_{b1}, respectively. Also, the whole gas state is given on the one side of the film. Within the duct, the gas volume fraction α_b changes from α_{b0} to α_{b1} and represents the change of the area of cross-section. The gas flow in the duct is governed by the relations (3.1). Using the similarity between (3.1) and (4.5), we can repeat the classical analysis of [7] to obtain the equality

$$\frac{d\alpha_b}{\alpha_b} = \left(\frac{v^2}{c_b^2} - 1\right)\frac{dv}{v}, \tag{4.6}$$

where now $v = u_b - u_a$ is the gas velocity relative to the velocity of the solid contact, and c_b is the gas sound speed.

We can easily establish several properties of this pore flow. Firstly, we know that the flow is isentropic, see (3.1b). Therefore, *no shocks are allowed in the flow*. For simplicity, let the relative velocity v be positive, $v > 0$. The case of negative v can be considered analogously. Then, from (4.6) we can state that *for increasing α_b the relative speed v increases when $v^2 > c_b^2$ and decreases when $v^2 < c_b^2$*. Using (3.1), we conclude that *in the direction of increasing α_b the gas flow is expanded when it is supersonic, and compressed when it is subsonic*. Finally, the *gas flow relative to the solid contact is supersonic (subsonic) at the one side of the solid contact, iff it is also supersonic (subsonic) at the other side of it*. To see this, consider the different cases in the proof of Theorem 3.4. It is convenient to represent these results in the following table, where ↑ denotes increase, and ↓ decrease:

Supersonic	$\alpha_b \uparrow$	$v \uparrow$	$\rho_b \downarrow$	$c_b \downarrow$
	$\alpha_b \downarrow$	$v \downarrow$	$\rho_b \uparrow$	$c_b \uparrow$
Subsonic	$\alpha_b \uparrow$	$v \downarrow$	$\rho_b \uparrow$	$c_b \uparrow$
	$\alpha_b \downarrow$	$v \uparrow$	$\rho_b \downarrow$	$c_b \downarrow$

Note that the duct can have several throats, see Fig. 3. By the classical theory of Laval nozzle, see e.g. [7], the gas flow can change its type from subsonic to supersonic and vice versa only at the throat. From the property established above, we conclude that this change can occur only an *even* number of times.

To summarize, we have rigorously shown the role of the non-conservative terms on the right-hand side of the homogeneous BN model (2.1), which was previously stated by Embid and Baer [11] and Bdzil et. al. [6] from physical considerations. Namely, the gas volume fraction measures the *porosity* of the solid phase. Then, *the change in porosity acts as a nozzle which can either accelerate or decelerate the gas flow*.

5. Weak solution to the Riemann problem

As we have mentioned in Section 2, one cannot define a weak solution to the system (2.1) as it is done for systems of conservation laws. The reason is that the system (2.5) cannot be written in divergence form. For the Riemann problem (2.1) and (2.3), however, this difficulty appears only along one line, namely the solid contact, where the volume fraction α_a is discontinuous. In the rest of domain, the volume fraction is constant and equal to its left or right value. Therefore, everywhere away from the solid contact the system (2.1) reduces to the system of *conservation laws*

$$\mathbf{u}_t + \mathbf{f}(\mathbf{u})_x = 0, \tag{5.1}$$

where

$$\mathbf{u} = \begin{bmatrix} \rho_a \\ \rho_a u_a \\ \rho_a E_a \\ \rho_b \\ \rho_b u_b \\ \rho_b E_b \end{bmatrix}, \quad \mathbf{f}(\mathbf{u}) = \begin{bmatrix} \rho_a u_a \\ \rho_a u_a^2 + p_a \\ u_a(\rho_a E_a + p_a) \\ \rho_b u_b \\ \rho_b u_b^2 + p_b \\ u_b(\rho_b E_b + p_b) \end{bmatrix}. \tag{5.2}$$

Note that this system is just the two sets of decoupled Euler equations for the phase a and b. For the system (5.1), we can define a weak solution in the usual manner, see Definition 5.2.

Let us look for a conservative system of equations such that the Rankine–Hugoniot relations for this system are exactly (3.1). We will investigate, to which system does the original system (2.1) reduce under the conditions (3.1a) and (3.1b). Using $u_a = \text{const.}$ in (2.1), we get

$$\frac{\partial \alpha_a}{\partial t} + \frac{\partial u_a \alpha_a}{\partial x} = 0, \tag{5.3a}$$

$$\frac{\partial \alpha_a \rho_a}{\partial t} + \frac{\partial \alpha_a \rho_a u_a}{\partial x} = 0, \tag{5.3b}$$

$$(p_a - p_b)\frac{\partial \alpha_a}{\partial x} + \alpha_a \frac{\partial p_a}{\partial x} = 0, \tag{5.3c}$$

$$\frac{\partial p_a}{\partial t} + \frac{\partial u_a p_a}{\partial x} = 0, \tag{5.3d}$$

$$\frac{\partial \alpha_b \rho_b}{\partial t} + \frac{\partial \alpha_b \rho_b u_b}{\partial x} = 0, \tag{5.3e}$$

$$\frac{\partial \alpha_b \rho_b u_b}{\partial t} + \frac{\partial(\alpha_b \rho_b u_b^2 + \alpha_b p_b)}{\partial x} = -p_b \frac{\partial \alpha_a}{\partial x}, \tag{5.3f}$$

$$\frac{\partial \alpha_b \rho_b E_b}{\partial t} + \frac{\partial \alpha_b u_b(\rho_b E_b + p_b)}{\partial x} = p_b u_a \frac{\partial \alpha_a}{\partial x}. \tag{5.3g}$$

Using (5.3c) and (5.3d) in (5.3f) and (5.3g), we obtain

$$\frac{\partial \alpha_b \rho_b u_b}{\partial t} + \frac{\partial(\alpha_b \rho_b u_b^2 + \alpha_a p_a + \alpha_b p_b)}{\partial x} = 0, \tag{5.4}$$

$$\frac{\partial(\alpha_b \rho_b E_b - \alpha_a p_a)}{\partial t} + \frac{\partial \alpha_b u_b(\rho_b E_b + p_b)}{\partial x} = 0. \tag{5.5}$$

Also, Eq. (5.3g) is equivalent to

$$\frac{\partial \eta_b}{\partial t} + u_b \frac{\partial \eta_b}{\partial x} = 0. \tag{5.6}$$

It is an easy matter to check that the system

$$\frac{\partial \alpha_a}{\partial t} + \frac{\partial u_a \alpha_a}{\partial x} = 0, \tag{5.7a}$$

$$\frac{\partial \alpha_a \rho_a}{\partial t} + \frac{\partial \alpha_a \rho_a u_a}{\partial x} = 0, \tag{5.7b}$$

$$\frac{\partial p_a}{\partial t} + \frac{\partial u_a p_a}{\partial x} = 0, \tag{5.7c}$$

$$\frac{\partial \alpha_b \rho_b}{\partial t} + \frac{\partial \alpha_b \rho_b u_b}{\partial x} = 0, \tag{5.7d}$$

$$\frac{\partial \alpha_b \rho_b u_b}{\partial t} + \frac{\partial(\alpha_b \rho_b u_b^2 + \alpha_a p_a + \alpha_b p_b)}{\partial x} = 0, \tag{5.7e}$$

$$\frac{\partial(\alpha_b \rho_b E_b - \alpha_a p_a)}{\partial t} + \frac{\partial \alpha_b u_b(\rho_b E_b + p_b)}{\partial x} = 0, \tag{5.7f}$$

$$\frac{\partial \eta_b}{\partial t} + u_b \frac{\partial \eta_b}{\partial x} = 0 \tag{5.7g}$$

is equivalent to the system (5.3) when $u_a = \text{const}$. Posing also the condition (3.1b), $\eta_b = \text{const.}$, Eqs. (5.3g) and (5.7g) drop off. Thus, the original *non-conservative* system (2.1) is equivalent to the *conservative* system

$$\frac{\partial \mathbf{U}}{\partial t} + \frac{\partial \mathbf{F}(\mathbf{U}, u_a)}{\partial x} = 0, \tag{5.8}$$

with

$$\mathbf{U} = \begin{bmatrix} \alpha_a \\ \alpha_a \rho_a \\ p_a \\ \alpha_b \rho_b \\ \alpha_b \rho_b u_b \\ \alpha_b \rho_b E_b - \alpha_a p_a \end{bmatrix}, \quad \mathbf{F}(\mathbf{U}, u_a) = \begin{bmatrix} \alpha_a u_a \\ \alpha_a \rho_a u_a \\ p_a u_a \\ \alpha_b \rho_b u_b \\ \alpha_b \rho_b u_b^2 + \alpha_a p_a + \alpha_b p_b \\ \alpha_b u_b(\rho_b E_b + p_b) \end{bmatrix} \tag{5.9}$$

under the conditions (3.1a) and (3.1b).

The Rankine–Hugoniot relations for the system (5.8) across the solid contact are

$$u_{\mathrm{a}}(\mathbf{U}_1 - \mathbf{U}_0) = \mathbf{F}_1 - \mathbf{F}_0, \tag{5.10}$$

where $\mathbf{U}$ and $\mathbf{F}$ are given by (5.9). Under the conditions (3.1a) and (3.1b), the relations (5.10) are equivalent to

$$\begin{aligned}
&u_{\mathrm{a}}(\alpha_{\mathrm{b}1}\rho_{\mathrm{b}1} - \alpha_{\mathrm{b}0}\rho_{\mathrm{b}0}) = \alpha_{\mathrm{b}1}\rho_{\mathrm{b}1}u_{\mathrm{b}1} - \alpha_{\mathrm{b}0}\rho_{\mathrm{b}0}u_{\mathrm{b}0},\\
&u_{\mathrm{a}}(\alpha_{\mathrm{b}1}\rho_{\mathrm{b}1}u_{\mathrm{b}1} - \alpha_{\mathrm{b}0}\rho_{\mathrm{b}0}u_{\mathrm{b}0}) = (P_1 + \alpha_{\mathrm{b}1}\rho_{\mathrm{b}1}u_{\mathrm{b}1}^2) - (P_0 + \alpha_{\mathrm{b}0}\rho_{\mathrm{b}0}u_{\mathrm{b}0}^2),\\
&u_{\mathrm{a}}[(\alpha_{\mathrm{b}1}\rho_{\mathrm{b}1}E_{\mathrm{b}1} - \alpha_{\mathrm{a}1}p_{\mathrm{a}1}) - (\alpha_{\mathrm{b}0}\rho_{\mathrm{b}0}E_{\mathrm{b}0} - \alpha_{\mathrm{a}0}p_{\mathrm{a}0})] = \alpha_{\mathrm{b}1}u_{\mathrm{b}1}(\rho_{\mathrm{b}1}E_{\mathrm{b}1} + p_{\mathrm{b}1}) - \alpha_{\mathrm{b}0}u_{\mathrm{b}0}(\rho_{\mathrm{b}0}E_{\mathrm{b}0} + p_{\mathrm{b}0}).
\end{aligned} \tag{5.11}$$

It is easy to see that the conditions (3.1a) and (3.1b) together with (5.11) are equivalent to the relations (3.1), expressing the constancy of the Riemann invariants across the solid contact.

Next, let us define a weak solution to the Riemann problem for a conservation law

$$\mathbf{u}_t + \mathbf{f}(\mathbf{u})_x = 0, \quad \mathbf{u}(x,0) = \begin{cases} \mathbf{u}_{\mathrm{L}}, & x \leqslant 0,\\ \mathbf{u}_{\mathrm{R}}, & x > 0. \end{cases} \tag{5.12}$$

As usual, we consider the self-similar solutions, i.e.,

$$\mathbf{u}(x,t) = \mathbf{u}(\xi), \quad \xi = \frac{x}{t}.$$

Then, the Riemann problem (5.12) is equivalent to

$$-\mathbf{u}_\xi\xi + \mathbf{f}(\mathbf{u})_\xi = 0, \quad \mathbf{u}(-\infty) = \mathbf{u}_{\mathrm{L}}, \quad \mathbf{u}(\infty) = \mathbf{u}_{\mathrm{R}}. \tag{5.13}$$

Let us suppose for the moment, that $\mathbf{u}$ is a classical solution of (5.13). Denote by $S(\xi_0,\xi_1)$ the sector, bounded by the rays ξ_0 and ξ_1. Also, let $C_0^1(]\xi_0,\xi_1[)$ be the class of all test functions ϕ which vanish outside of the open interval $]\xi_0,\xi_1[$. We multiply (5.13) by ϕ and integrate over all ξ,

$$\int_{-\infty}^{\infty}(-\mathbf{u}_\xi\xi + \mathbf{f}(\mathbf{u})_\xi)\phi(\xi)\,\mathrm{d}\xi = \int_{\xi_0}^{\xi_1}(-\mathbf{u}_\xi\xi + \mathbf{f}(\mathbf{u})_\xi)\phi(\xi)\,\mathrm{d}\xi.$$

Integrating by parts gives

$$\int_{\xi_0}^{\xi_1}(-\mathbf{u}_\xi\xi+\mathbf{f}(\mathbf{u})_\xi)\phi\,\mathrm{d}\xi=(-\xi\phi\mathbf{u}+\phi\mathbf{f}(\mathbf{u}))|_{\xi_0}^{\xi_1}+\int_{\xi_0}^{\xi_1}(\mathbf{u}(\phi\xi)_\xi-\mathbf{f}(\mathbf{u})\phi_\xi)\,\mathrm{d}\xi=\int_{\xi_0}^{\xi_1}(\mathbf{u}(\phi\xi)_\xi-\mathbf{f}(\mathbf{u})\phi_\xi)\,\mathrm{d}\xi=0. \tag{5.14}$$

Thus, if $\mathbf{u}$ is a classical solution of (5.13), then (5.14) holds true for all $\phi \in C_0^1(]\xi_0,\xi_1[)$. However, $\mathbf{u}$ does not need to be differentiable anymore. This gives rise to the following definition.

Definition 5.1. A bounded measurable function $\mathbf{u} = \mathbf{u}(\xi)$ is called a weak solution to the Riemann problem (5.13) in a sector $S(\xi_0,\xi_1)$ if $\mathbf{u}$ satisfies (5.14) for all $\phi \in C_0^1(]\xi_0,\xi_1[)$.

Let us check, if we can get the Rankine–Hugoniot conditions across a discontinuity from this definition. Consider a ray of discontinuity s and a sector $S(s_0,s_1)$ such that $s \in S(s_0,s_1)$ and s is the only discontinuity there. Let $\phi \in C_0^1(]s_0,s_1[)$ be some test function. The weak solution of (5.13) in $S(s_0,s_1)$ is defined by

$$\int_{s_0}^{s_1} (\mathbf{u}(\phi\xi)_\xi - \mathbf{f}(\mathbf{u})\phi_\xi)\,\mathrm{d}\xi = 0.$$

Splitting the integral and integrating by parts,

$$\begin{aligned}\int_{s_0}^{s_1} (\mathbf{u}(\phi\xi)_\xi - \mathbf{f}(\mathbf{u})\phi_\xi)\,\mathrm{d}\xi &= \int_{s_0}^{s} (\mathbf{u}(\phi\xi)_\xi - \mathbf{f}(\mathbf{u})\phi_\xi)\,\mathrm{d}\xi + \int_{s}^{s_1} (\mathbf{u}(\phi\xi)_\xi - \mathbf{f}(\mathbf{u})\phi_\xi)\,\mathrm{d}\xi \\ &= (-\xi\phi\mathbf{u} + \phi\mathbf{f}(\mathbf{u}))|_{s_0}^{s} + \int_{s_0}^{s} (-\mathbf{u}_\xi\xi + \mathbf{f}(\mathbf{u})_\xi)\phi\,\mathrm{d}\xi + (-\xi\phi\mathbf{u} + \phi\mathbf{f}(\mathbf{u}))|_{s}^{s_1} \\ &\quad + \int_{s}^{s_1} (-\mathbf{u}_\xi\xi + \mathbf{f}(\mathbf{u})_\xi)\phi\,\mathrm{d}\xi \\ &= \phi(s)s(\mathbf{u}_\mathrm{l} - \mathbf{u}_\mathrm{r}) + \phi(s)(\mathbf{f}(\mathbf{u}_\mathrm{r}) - \mathbf{f}(\mathbf{u}_\mathrm{l})) = 0, \end{aligned} \tag{5.15}$$

where $\mathbf{u}_\mathrm{l} = \mathbf{u}(s-0)$ and $\mathbf{u}_\mathrm{r} = \mathbf{u}(s+0)$. Dividing (5.15) by $\phi(s) \neq 0$, we obtain the usual Rankine–Hugoniot relations across s.

Now, using Definition 5.1, we can define a weak solution to the Riemann problem for the *non-conservative* system (2.1). We will utilize the above established fact that everywhere locally this non-conservative system is equivalent to the conservative one, either (5.1) or (5.8).

Definition 5.2. Consider a sector $S(\xi_0, \xi_1)$, such that the solid contact lies in it, and assume that the solid contact is the only ray of discontinuity there. Then, a function $\mathbf{u} = \mathbf{u}(\xi) \in L^\infty_{\mathrm{loc}}(\mathbb{R})$ is called a weak solution of the Riemann problem (2.1) and (2.3), if for any small $\epsilon > 0$

1. To the left of $S(\xi_0, \xi_1)$, i.e., $\xi \in [-\infty, \xi_0]$,

$$\int_{-\infty}^{\xi_0} (\mathbf{u}(\phi\xi)_\xi - \mathbf{f}(\mathbf{u})\phi_\xi)\,\mathrm{d}\xi = 0, \quad \phi \in C_0^1(]-\infty, \xi_0 + \epsilon[),$$

   $\mathbf{u}(\xi) = \mathbf{u}(x,t)$, $\mathbf{f}(\mathbf{u}) = \mathbf{f}(\mathbf{u})$, and $\mathbf{u}$, $\mathbf{f}(\mathbf{u})$ are given by (5.2).
2. To the right of $S(\xi_0, \xi_1)$, i.e., $\xi \in [\xi_1, \infty]$,

$$\int_{\xi_1}^{\infty} (\mathbf{u}(\phi\xi)_\xi - \mathbf{f}(\mathbf{u})\phi_\xi)\,\mathrm{d}\xi = 0, \quad \phi \in C_0^1(]\xi_1 - \epsilon, \infty[),$$

   $\mathbf{u}(\xi) = \mathbf{u}(x,t)$, $\mathbf{f}(\mathbf{u}) = \mathbf{f}(\mathbf{u})$, and $\mathbf{u}$, $\mathbf{f}(\mathbf{u})$ are given by (5.2).
3. Inside of $S(\xi_0, \xi_1)$, i.e., $\xi \in [\xi_0, \xi_1]$,

$$\int_{\xi_0}^{\xi_1} (\mathbf{u}(\phi\xi)_\xi - \mathbf{f}(\mathbf{u})\phi_\xi)\,\mathrm{d}\xi = 0, \quad \phi \in C_0^1(]\xi_0 - \epsilon, \xi_1 + \epsilon[),$$

   $\mathbf{u}(\xi) = \mathbf{U}(x,t)$, $\mathbf{f}(\mathbf{u}) = \mathbf{F}(\mathbf{U}, u_\mathrm{a})$, and $\mathbf{U}$, $\mathbf{F}(\mathbf{U}, u_\mathrm{a})$ are given by (5.9).

Remark 1. Note that in the sector $S(\xi_0 - \epsilon, \xi_0 + \epsilon)$, Definitions 1 and 3 coincide, and in the sector $S(\xi_1 - \epsilon, \xi_1 + \epsilon)$, Definitions 2 and 3 coincide.

Remark 2. In [9], Dal Maso et al. introduce a notion of the non-conservative product and give a definition of a weak solution to a general non-conservative system on its basis. In particular, this applies also to the system (2.1). In contrast to the definition of [9], we have used some physical observations in Definition 5.2, which are valid only for systems of a certain structure like (2.1). We believe that our definition may give an idea for constructing of approximate Riemann solvers for non-conservative systems like (2.1).

6. "Inverse" solution to the Riemann problem

Consider the Riemann problem (2.1) and (2.3). Since the system (2.1) has six distinct characteristic speeds (2.7), the solution to the Riemann problem (2.1) and (2.3) is composed of at most six waves, namely shocks, rarefactions, and contacts for the two phases $k = \mathrm{a}, \mathrm{b}$. These waves separate at most seven constant states in the solution of the Riemann problem. Remember that the system (2.1) is non-strictly hyperbolic, so some waves can coincide or overlap with each other.

The exact solution to the Riemann problem (2.1) and (2.3) is obtained as follows: For given end states $\mathbf{u}_\mathrm{L}, \mathbf{u}_\mathrm{R}$, one looks for admissible waves such that they connect $\mathbf{u}_\mathrm{L}$ with $\mathbf{u}_\mathrm{R}$ in the phase space. However, a corresponding numerical procedure would be very complicated. Indeed, the wave speeds in the solution of the Riemann problem (2.1) and (2.3) cannot be ordered a priori. Therefore, one has to consider several possible cases. Analogous to the results of [2], we expect that the exact solution to the Riemann problem (2.1) and (2.3) can be reduced to the solution of a system of nonlinear algebraic equations, which can be solved with some iterative method.

Here, we do not pursue the goal to solve the Riemann problem (2.1) and (2.3) in the "direct" way described above. Instead, we prescribe the configuration of the Riemann problem, i.e., the mutual position of the waves, and look for the end states $\mathbf{u}_\mathrm{L}$ and $\mathbf{u}_\mathrm{R}$, which are compatible with it. In other words, we construct the exact solution to the Riemann problem. In what follows, we will refer to this procedure as the "*inverse*" *solution* of the Riemann problem (2.1) and (2.3).

To be more precise, we fix the configuration of the Riemann problem as follows. We choose the intermediate state $\mathbf{u}_0$ to the left of the solid contact Σ, and fix the volume fractions to the left and to the right of Σ. Further, we prescribe which waves should be to the left of Σ, and which to the right. Depending on the wave, we determine its position by specifying the following quantities:

- Shock: given shock speed s, family
- Rarefaction: given pressure behind, family
- Contact: given density behind.

This process is illustrated in Fig. 4. In the procedure of constructing the exact solution we exclude the cases, in which some gas waves coincide with the solid contact Σ. The case of coinciding waves requires special investigation and will be addressed in Section 8. As we have seen in Section 5, the system (2.1) reduces to

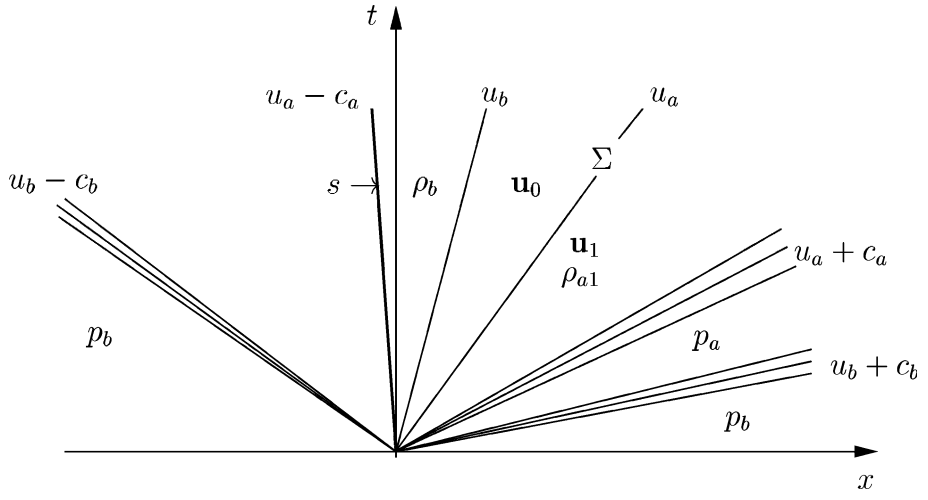

Fig. 4. "Inverse" solution of the Riemann problem.

the two sets of the usual Euler equations (5.1) away from the solid contact Σ. Therefore, we can use the usual admissibility conditions on the waves there. For the solid contact 0-wave, we use the evolutionarity criterion of Section 3.4.

The procedure of constructing the exact solution to the Riemann problem for the homogeneous BN model (2.1) has been implemented in a software package CONSTRUCT [1]. With its help, we CONSTRUCTed several test cases for the system (2.1), see Section 9. We hope that these tests will be helpful in assessing numerical methods for non-conservative systems of the type (2.1). Our idea is that interested researches can try their numerical methods on Riemann problems for the homogeneous BN model (2.1), and compare the numerical results with exact solutions.

In Section 4, we have shown that the Euler equations in a duct of variable cross-section (4.2) can be formally obtained from the homogeneous BN model (2.1) under conditions (4.3) and (4.4). Consequently, one can CONSTRUCT [1] the exact solution to the Riemann problem for the system (4.2) exactly as it is done for the homogeneous BN model (2.1). One just has to set the solid velocity u_a equal to zero, and consider only gas waves in the solution to the Riemann problem, cf. (4.3) and (4.4). In doing so, we can get test problems for numerical methods for the Euler equations in the duct. See Section 9 for an example.

7. Non-uniqueness of the Riemann solution

Obviously, for a given configuration of the Riemann problem to (2.1), we find the corresponding initial data (2.3) uniquely. However, for certain initial data (2.3), the configuration of the Riemann problem *cannot* be determined uniquely. In other words, we can point out another configuration of the Riemann problem to (2.1), such that it will correspond to the same initial data (2.3). Moreover, for certain initial data the solution to the Riemann problem (2.1) and (2.3) does not exist. To show this, we will use the analogies between the homogeneous BN model (2.1) and the Euler equations in a duct (4.2), established in Section 4.

The system (4.2) belongs to a class of *resonant* hyperbolic systems, see Isaacson and Temple [15,16]. In [4], we provide an analysis of the Riemann problem for the system (4.2) and show that for certain initial data, its solution is non-unique. Also, for some initial data, the Riemann problem for (4.2) does not have a solution. Since the system (4.2) can be formally obtained from the homogeneous BN model (2.1) under conditions (4.3) and (4.4), the same is true for the Riemann problem (2.1) and (2.3). In [4], we propose an admissibility criterion in order to rule out non-physical solutions to the Riemann problem for the Euler equations in a duct (4.2). However, its detailed investigation, as well as its use for the homogeneous BN model (2.1) is an open question.

8. Coinciding waves

As we mentioned previously, the wave speeds in the solution to the Riemann problem (2.1) and (2.3) can coincide with each other. Namely, each of the solid waves, associated with the eigenvalues

$$\lambda_1 = u_a - c_a, \quad \lambda_0 = \lambda_2 = u_a, \quad \lambda_3 = u_a + c_a$$

can coincide with either of gas waves, associated with the eigenvalues

$$\lambda_4 = u_b - c_b, \quad \lambda_5 = u_b, \quad \lambda_6 = u_b + c_b.$$

However, the solid variables do not change across the gas 4-, 5-, and 6-waves, and the gas variables do not change across the solid 1- and 3-waves, see Section 2. Therefore, the potentially interesting cases arise only when the solid contact 0-wave coincides with either a gas 4-, 5-, or 6-wave. Since the gas 4- and 6-waves can be either rarefactions or shock waves, and the gas 5-wave is a contact discontinuity, we will consider these three cases separately.

8.1. Coinciding contacts

Consider the situation when the gas contact approaches the solid contact Σ from the right. The case when the gas contact approaches Σ from the left can be handled analogously. Denote the states, separated by the contacts, with $\mathbf{u}_0$, $\mathbf{u}_1$, and $\mathbf{u}$, and the phase variables in these states with subscript 0, 1, and no subscript respectively, see Fig. 5. Across the contacts, the corresponding Riemann invariants are constant, see Section 2. Therefore

$$\alpha_k \equiv \alpha_{k1}, \quad \rho_{\mathrm{a}} \equiv \rho_{\mathrm{a}1}, \quad u_k \equiv u_{k1}, \quad p_k \equiv p_{k1}, \quad k = \mathrm{a}, \mathrm{b}, \tag{8.1}$$

but in general $\rho_{\mathrm{b}} \neq \rho_{\mathrm{b}1}$. Also, $u_{\mathrm{a}0} \equiv u_{\mathrm{a}1} \equiv u_{\mathrm{a}}$.

We fix the state $\mathbf{u}_0$ and the volume fractions to the right of Σ. The gas contact will approach Σ from the right if

$$u_{\mathrm{b}1} + \epsilon = u_{\mathrm{a}}, \quad \epsilon \to -0. \tag{8.2}$$

We wish to investigate how will the gas variables in $\mathbf{u}$ change; the values of the solid variables in $\mathbf{u}$ coincide with those in $\mathbf{u}_1$, see (8.1).

The state $\mathbf{u}_1$ is determined by the admissible root of (3.3),

$$F(\rho_{\mathrm{b}1}) = \frac{1}{2}\left(\frac{M}{\alpha_{\mathrm{b}1}\rho_{\mathrm{b}1}}\right)^2 + \frac{\gamma_{\mathrm{b}}\eta_{\mathrm{b}}\rho_{\mathrm{b}1}^{\gamma_{\mathrm{b}}-1}}{\gamma_{\mathrm{b}}-1} - E = 0. \tag{8.3}$$

By (8.2) and (3.5), we observe that the function $F(\rho_{\mathrm{b}1})$ reaches its minimum at the point

$$\rho_* = \left(\frac{\alpha_{\mathrm{b}0}^2\rho_{\mathrm{b}0}^2}{\alpha_{\mathrm{b}1}^2\gamma_{\mathrm{b}}\eta_{\mathrm{b}}}\epsilon^2\right)^{(1/(\gamma_{\mathrm{b}}+1))} \to 0, \quad \epsilon \to +0.$$

Thus, the smallest of two roots $\rho_{\mathrm{b}1} = \tilde{\rho}_{\mathrm{b}1}$ of the Eq. (8.3) becomes infinitesimal,

$$\rho_{\mathrm{b}1} \to 0, \quad \epsilon \to +0,$$

cf. Fig. 1. Let us show that this root is not admissible. Indeed, according to (8.2) $u_{\mathrm{b}1} > u_{\mathrm{a}}$, so by (3.1c) also $u_{\mathrm{b}0} > u_{\mathrm{a}}$. Therefore, there are precisely two gas characteristics which impinge on Σ from the left, see Fig. 5. In order for Σ to be evolutionary, there must be one gas characteristic which impinges on it from the right, see Theorem 3.3. This is equivalent to

$$u_{\mathrm{b}1} - c_{\mathrm{b}1} < u_{\mathrm{a}}.$$

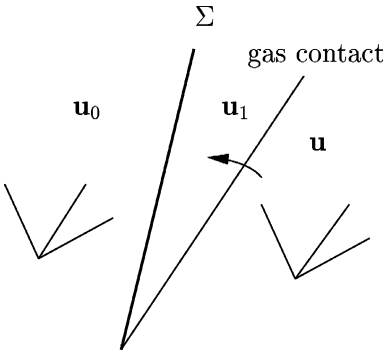

Fig. 5. Gas contact approaches Σ from the right. Two gas characteristics impinge on Σ from the left, and one from the right.

Since $u_{b1} > u_a$, one can rewrite this condition as

$$(u_{b1} - u_a)^2 - c_{b1}^2 < 0. \tag{8.4}$$

Using this in (3.1e), one has

$$(u_{b1} - u_a)^2 - c_{b1}^2 = 2E - \frac{\gamma_b + 1}{\gamma_b - 1} c_{b1}^2 = 2E - \frac{\gamma_b + 1}{\gamma_b - 1} \eta \gamma_b \rho_{b1}^{\gamma_b - 1} < 0.$$

This inequality will be fulfilled iff ρ_{b1} exceeds some positive constant, i.e.,

$$\eta \gamma_b \rho_{b1}^{\gamma_b - 1} > \frac{\gamma_b - 1}{\gamma_b + 1} 2E. \tag{8.5}$$

Therefore, the root $\rho_{b1} \to 0$ is not admissible, and we can restrict ourselves only to the values of ρ_{b1} which satisfy the condition (8.5). For such ρ_{b1} Eqs. (3.1c) and (8.2) imply that

$$u_{b1} \to u_a. \tag{8.6}$$

Let us rewrite (3.1e) as follows

$$\frac{(u_{b0} - u_a)^2}{2} + \frac{\gamma_b \eta_b \rho_{b0}^{\gamma_b - 1}}{\gamma_b - 1} = \frac{(u_{b1} - u_a)^2}{2} + \frac{\gamma_b \eta_b \rho_{b1}^{\gamma_b - 1}}{\gamma_b - 1}. \tag{8.7}$$

Using (8.2) and (8.6) in (8.7), we have

$$\rho_{b1} \to \rho_{b0}. \tag{8.8}$$

Finally using (8.8) in (3.1b), we have

$$p_{b1} \to p_{b0}. \tag{8.9}$$

Since by (8.1) $u_b \equiv u_{b1}$ and $p_b \equiv p_{b1}$, we have

$$u_b \to u_a \quad p_b \to p_{b0}. \tag{8.10}$$

To summarize, we have proved the following theorem.

Theorem 8.1. *Consider the situation when the gas contact approaches the solid contact from the right, i.e.* $u_{b1} + \epsilon = u_a$, $\epsilon \to -0$. *Then the gas pressure to the right of the solid contact approaches the corresponding value to the left of it*,

$$p_b \equiv p_{b1} \to p_{b0}.$$

At the limit,

$$p_b \equiv p_{b1} = p_{b0}.$$

8.2. Shock vs. solid contact

Finally, we describe the behaviour of the solution, when an admissible gas shock wave approaches the solid contact Σ. Here, we consider the shock to the right of Σ, i.e.,

$$s \to u_a, \quad s > u_a, \tag{8.11}$$

where s is the shock speed. The case when the shock approaches Σ from the left can be handled analogously.

Denote the states, separated by Σ and the shock, with $\mathbf{u}_0$, $\mathbf{u}_1$, and $\mathbf{u}$, and the phase variables in these states with subscript 0, 1, and no subscript, respectively. Thus the notations are analogous to the case when a gas contact approaches the solid contact, see Fig. 5.

Similar to the case of approaching contacts, see Section 8.1, we fix the state $\mathbf{u}_0$ and the volume fractions to the right of Σ. We wish to investigate how will the gas variables in $\mathbf{u}$ change; the values of the solid variables in $\mathbf{u}$ coincide with those in $\mathbf{u}_1$, see Section 2.

Across the solid contact Σ, the Riemann invariants (3.1) are constant. Across the shock, the Rankine–Hugoniot conditions are

$$\begin{aligned}
&\rho_{b1}(u_{b1}-s)=\rho_b(u_b-s),\\
&\rho_{b1}(u_{b1}-s)^2+p_{b1}=\rho_b(u_b-s)^2+p_b,\\
&\frac{(u_{b1}-s)^2}{2}+\frac{c_{b1}^2}{\gamma_b-1}=\frac{(u_b-s)^2}{2}+\frac{c_b^2}{\gamma_b-1}.
\end{aligned} \tag{8.12}$$

Using (8.11) and (3.1) in (8.12), we get

$$\rho_{b1}(u_b-s)\to\frac{M}{\alpha_{b1}}=:M_1, \tag{8.13a}$$

$$\rho_{b1}(u_b-s)^2+p_b\to\frac{1}{\alpha_{b1}}(P-\alpha_{a1}p_{a1})=:P_1, \tag{8.13b}$$

$$\frac{(u_b-s)^2}{2}+\frac{c_b^2}{\gamma_b-1}\to E. \tag{8.13c}$$

Multiply (8.13c) by $2\rho_b$, and substract the result from (8.13b). Then

$$p_b\frac{\gamma_b+1}{1-\gamma_b}-\frac{2\gamma_b\pi_b}{\gamma_b-1}\to P_1-2\rho_bE. \tag{8.14}$$

From (8.13a) and (8.13b), we have

$$p_b\to P_1-\frac{M_1^2}{\rho_b}.$$

Substituting this into (8.14), we get the following relation for ρ_b,

$$\left(P_1-\frac{M_1^2}{\rho_b}\right)\frac{\gamma_b+1}{1-\gamma_b}-\frac{2\gamma_b\pi_b}{\gamma_b-1}\to P_1-2\rho_bE.$$

In the limit, it reveals the quadratic equation for ρ_b,

$$2E(\gamma_b-1)\rho_b^2-2\gamma_b(P_1+\pi_b)\rho_b+M_1^2(\gamma_b+1)=0. \tag{8.15}$$

This equation has two roots. One of them is always ρ_{b0}, and corresponds to the trivial solution when $\mathbf{u}\equiv\mathbf{u}_1$, so that the shock wave between $\mathbf{u}$ and $\mathbf{u}_1$ disappears. Therefore, we take the other root of (8.15). Using this root in (8.13), we find the gas velocity and pressure in $\mathbf{u}$ as follows:

$$u_{\mathrm{b}} = \frac{M_1}{\rho_{\mathrm{b}}} + s,$$
$$p_{\mathrm{b}} = P_1 - \frac{M_1^2}{\rho_{\mathrm{b}}}. \tag{8.16}$$

Thus, we see that the state behind the shock approaches some finite state with the gas variables given by (8.16), as the shock approaches the solid contact.

8.3. Sonic state attached to the solid contact

When either of gas characteristic speeds $\lambda_{1,3} = u_{\mathrm{b}} \mp c_{\mathrm{b}}$ coincides with the solid contact speed $\lambda_0 = \lambda_2 = u_{\mathrm{a}}$, the homogeneous BN model (2.1) becomes parabolic degenerate, cf. (2.8). Such situation arises when a gas 1- or 3-characteristic approaches the solid contact

$$u_{\mathrm{b}} \mp c_{\mathrm{b}} \to u_{\mathrm{a}} \tag{8.17}$$

and in the limit touches it, $u_{\mathrm{b}} \mp c_{\mathrm{b}} = u_{\mathrm{a}}$.

In order to give an interpretation to the parabolic degeneracy conditions (2.8), we can use the analogy between the flow inside of the solid contact and in the converging-diverging nozzle, see Section 4. We can represent the solid contact as a porous film, such that each pore is a converging-diverging nozzle, see Fig. 3. The flow in the pore is governed by the relations (4.6). Consider the flow such the condition (8.17) holds at the cross-section $\alpha_{\mathrm{b}0}$, i.e., at the state $\mathbf{u}_0$ to the left of Σ. Then, the relative gas flow there is almost sonic,

$$M_0 = \frac{|\, u_{\mathrm{b}0} - u_{\mathrm{a}} \,|}{c_{\mathrm{b}0}} = 1 + \epsilon, \quad \epsilon \to \pm 0,$$

where M is the local relative Mach number. Depending on the sign of ϵ and on the difference $\alpha_{\mathrm{b}1} - \alpha_{\mathrm{b}0}$, the gas flow in the pore either accelerates and expands, or decelerates and compresses, leading to the very different states $\mathbf{u}_1$ to the right of Σ. Thus, such a sonic configuration is *not stable*.

We can also give an interpretation to the case when Eq. (3.3) has no roots. As it was mentioned in Section 3, this is the case when $\alpha_{\mathrm{b}1}$ becomes sufficiently small. According to the results of Section 4, the change of the gas parameters to the right of the solid contact is determined whether the gas relative speed $u_{\mathrm{b}} - u_{\mathrm{a}}$ is subsonic or supersonic. When it is subsonic, then the gas flow accelerates and expands, so the sound speed decreases and the relative Mach number $M = |u_{\mathrm{b}1} - u_{\mathrm{a}}|/c_{\mathrm{b}1}$ increases. As soon as the gas volume fraction falls below its critical value, where $M = 1$, a shock intervenes and the isentropic flow does not exist anymore. On the other hand, when the gas relative flow is supersonic, the relative Mach number decreases. Again, for the gas volume fraction below its critical value, the isentropic flow does not exist.

It is an easy matter to check that the solid contact can lie *inside* of the gas rarefaction only in the trivial case when $\alpha_{\mathrm{b}0} = \alpha_{\mathrm{b}1}$, i.e., when the phases a and b are decoupled. Indeed, let us consider the gas 1-rarefaction (the case of 3-rarefaction can be done analogously). In the 1-rarefaction wave the characteristic speed $u_{\mathrm{b}} - c_{\mathrm{b}}$ varies continuously, so on both sides of the solid contact with velocity u_{a}

$$u_{\mathrm{b}0} - c_{\mathrm{b}0} \to u_{\mathrm{a}}, \quad u_{\mathrm{b}1} - c_{\mathrm{b}1} \to u_{\mathrm{a}}$$

and at the limit

$$u_{\mathrm{b}0} - c_{\mathrm{b}0} = u_{\mathrm{a}}, \quad u_{\mathrm{b}1} - c_{\mathrm{b}1} = u_{\mathrm{a}}.$$

Using this in (3.1e), we get

$$c_{\mathrm{b}0} = c_{\mathrm{b}1}.$$

Combining this equality with (3.1b), we obtain that

$$\rho_{b0} = \rho_{b1}, \quad p_{b0} = p_{b1}.$$

Finally, from (3.1c) we have

$$\alpha_{b0} = \alpha_{b1}.$$

9. Test cases

As we have seen in Section 2, the homogeneous BN model (2.1) consists of the two sets of the Euler equations for both phases, coupled with the non-conservative terms. Therefore, a "good" numerical scheme for the system (2.1) should be necessarily "good" for the Euler equations. Here the notion "good" denotes the properties like convergence to the entropy solution, reasonable accuracy, robustness, etc. For the Euler equations, one has a number of test cases, intended to check these properties for each particular scheme. An excellent reference is Toro [29].

However, for the two-phase problems, there exists only a small number of test cases, and usually they incorporate several physical effects, specific material properties, and external forces, see e.g. [24]. All these make it difficult to compare numerical methods for two-phase flow problems.

Here, we propose a number of test cases using the exact solution to Riemann problems, which was obtained in Section 6. The exact solutions were found by running the package CONSTRUCT [1]. Remember that the procedure to construct exact solutions to the Riemann problem for both the homogeneous BN model (2.1) and the Euler in a duct (4.2) is essentially the same, see Section 6. Therefore, we can use CONSTRUCT [1] for the both systems (2.1) and (4.2).

Some tests presented below are designed to assess the behaviour of numerical methods for Riemann problems with almost coinciding wave speeds. As we shall shortly see, some methods can have hard time on such tests.

As an example, we test a numerical method for compressible multiphase flows which we have proposed in [3]. In what follows, it will be referred to as VFRoe, stands for *Volumes Finis Roe* in French. As it is clear from the name, it employs the features of both Roe's and finite volume methods. At each cell boundary, one solves the linearized Riemann problem as in the Roe's method. Then, we calculate the numerical flux function as the physical flux in the intermediate state of the solution of the Riemann problem. For the non-conservative terms, we use some physically motivated discretization, see [3] for details. In [3], we show the robustness and accuracy of the method on several numerical examples.

Here, we compare the numerical results of VFRoe with the exact solutions to the Riemann problems for the Euler equations in the duct of variable cross-section (4.2), and for the homogeneous BN model (2.1). To see clearly the effects of VFRoe discretization, we present here the numerical results of the first order accuracy. The extension to the second order is described in [3]. We have always used 300 mesh cells in the calculations below. For simplicity, we have used the ideal gas EOS, i.e., $\gamma_k = 1.4$ and $\pi_k = 0$ in (2.4), $k = \mathrm{a}, \mathrm{b}$. The initial position of the discontinuity is always 0.5.

9.1. Euler equations in the duct of variable cross-section

Consider the following Riemann problem:

A_L	ρ_L	v_L	p_l	A_R	ρ_R	v_R	p_R
0.6	0.96	1.0833	2.8333	0.7	1.7741	1.1187	4.0

The solution consists of the 1-shock, traveling to the left, stationary 0-wave corresponding to the jump in the cross-section, 2-contact, and the 3-rarefaction. The comparison of the numerical solution with the exact one is presented in Fig. 6.

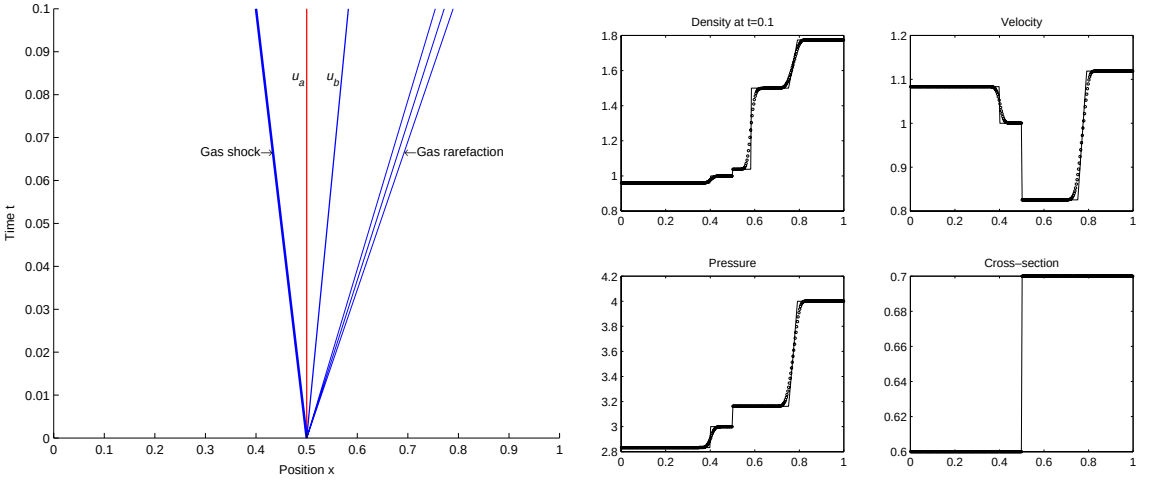

Fig. 6. The Riemann problem for the Euler equations in the duct of variable cross section.

9.2. Test cases for the BN model

Test 1: Single solid contact. Consider the following Riemann problem for the BN model:

Phase k	$\alpha_{k\mathrm{L}}$	$\rho_{k\mathrm{L}}$	$u_{k\mathrm{L}}$	$p_{k\mathrm{L}}$	$a_{k\mathrm{R}}$	$\rho_{k\mathrm{R}}$	$u_{k\mathrm{R}}$	$p_{k\mathrm{R}}$
a	0.8	2	0.3	5	0.3	2	0.3	12.8567
b	0.2	1	2	1	0.7	0.1941	2.8011	0.10

Its solution consists of the single solid contact, propagating with the velocity 0.3. The numerical results are presented in Fig. 7. In this test, the jump of the volume fraction $\alpha_{a\mathrm{R}} - \alpha_{a\mathrm{L}} = 0.5$.

Test 2: Coinciding shocks and rarefactions. A particular issue on the Riemann problem for Eqs. (2.1) is that several waves can coincide with each other. However, the gas parameters do not change across the solid waves (except of the solid contact) and vice versa, see Section 2. Thus, the numerical solution across these waves should be independent of the presence of the wave of the other phase. If we take the initial data as follows

Phase k	$\alpha_{k\mathrm{L}}$	$\rho_{k\mathrm{L}}$	$u_{k\mathrm{L}}$	$p_{k\mathrm{L}}$	$a_{k\mathrm{R}}$	$\rho_{k\mathrm{R}}$	$u_{k\mathrm{R}}$	$p_{k\mathrm{R}}$
a	0.1	0.2068	1.4166	0.0416	0.2	2.2263	0.9366	6.0
b	0.9	0.5806	1.5833	1.375	0.8	0.4890	−0.70138	0.986

then the Riemann solution consists of two coinciding 1-shock waves for the gas and solid, and the gas 3-shock inside of the solid 3-rarefaction. The structure of the Riemann problem and the numerical results for this test are presented in Fig. 8.

Test 3: Coinciding contacts. When the solid and gas contacts approach each other, both u_{a} and p_{b} are almost constant there, see Section 8.1. Therefore, the non-conservative terms

$$p_{\mathrm{b}}\frac{\partial \alpha_{\mathrm{a}}}{\partial x} \approx \frac{\partial p_{\mathrm{b}}\alpha_{\mathrm{a}}}{\partial x}, \quad p_{\mathrm{b}}u_{\mathrm{a}}\frac{\partial \alpha_{\mathrm{a}}}{\partial x} \approx \frac{\partial p_{\mathrm{b}}u_{\mathrm{a}}\alpha_{\mathrm{a}}}{\partial x}$$

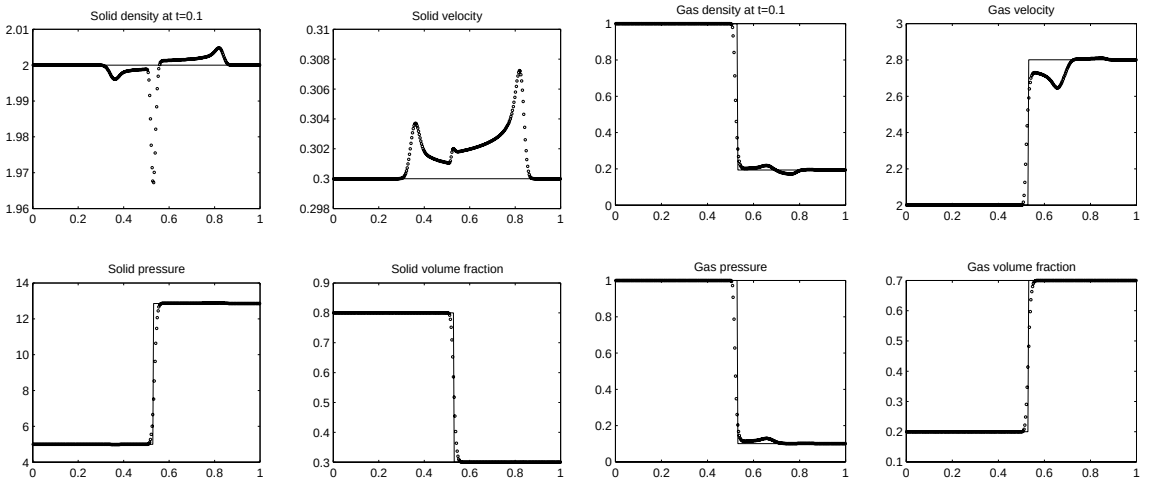

Fig. 7. The numerical results for Test 1.

near the solid contact. Thus, this test should not pose serious difficulties. This configuration occurs if we take the following initial data

Phase k	$\alpha_{k\mathrm{L}}$	$\rho_{k\mathrm{L}}$	$u_{k\mathrm{L}}$	$p_{k\mathrm{L}}$	$a_{k\mathrm{R}}$	$\rho_{k\mathrm{R}}$	$u_{k\mathrm{R}}$	$p_{k\mathrm{R}}$
a	0.1	0.9123	1.6305	1.5666	0.9	0.8592	−0.0129	1.1675
b	0.9	2.6718	−0.050	1.5	0.1	1.3359	0.5438	1.5

The structure of the Riemann problem and the numerical results for this test are presented in Fig. 9.

Test 4: Gas shock approaches solid contact. In the limit, i.e., when the gas shock coincides with the solid contact, the jump conditions across this ''double discontinuity'' are given in Section 8.2. To achieve such a configuration, one may take the following initial data

Phase k	$\alpha_{k\mathrm{L}}$	$\rho_{k\mathrm{L}}$	$u_{k\mathrm{L}}$	$p_{k\mathrm{L}}$	$a_{k\mathrm{R}}$	$\rho_{k\mathrm{R}}$	$u_{k\mathrm{R}}$	$p_{k\mathrm{R}}$
a	0.5	2.1917	−0.995	3.0	0.1	0.6333	−1.1421	2.5011
b	0.5	6.3311	−0.789	1	0.9	0.4141	−0.6741	0.0291

The structure of the Riemann problem and the numerical results for this case is presented in Fig. 10.

Test 5: Gas rarefaction attached to the solid contact. Consider the following Riemann problem

Phase k	$\alpha_{k\mathrm{L}}$	$\rho_{k\mathrm{L}}$	$u_{k\mathrm{L}}$	$p_{k\mathrm{L}}$	$a_{k\mathrm{R}}$	$\rho_{k\mathrm{R}}$	$u_{k\mathrm{R}}$	$p_{k\mathrm{R}}$
a	0.5	2	−1	2	0.1	1	−1	8.3994
b	0.5	0.2702	−3.4016	0.1	0.9	0.4666	−2.6667	0.2148

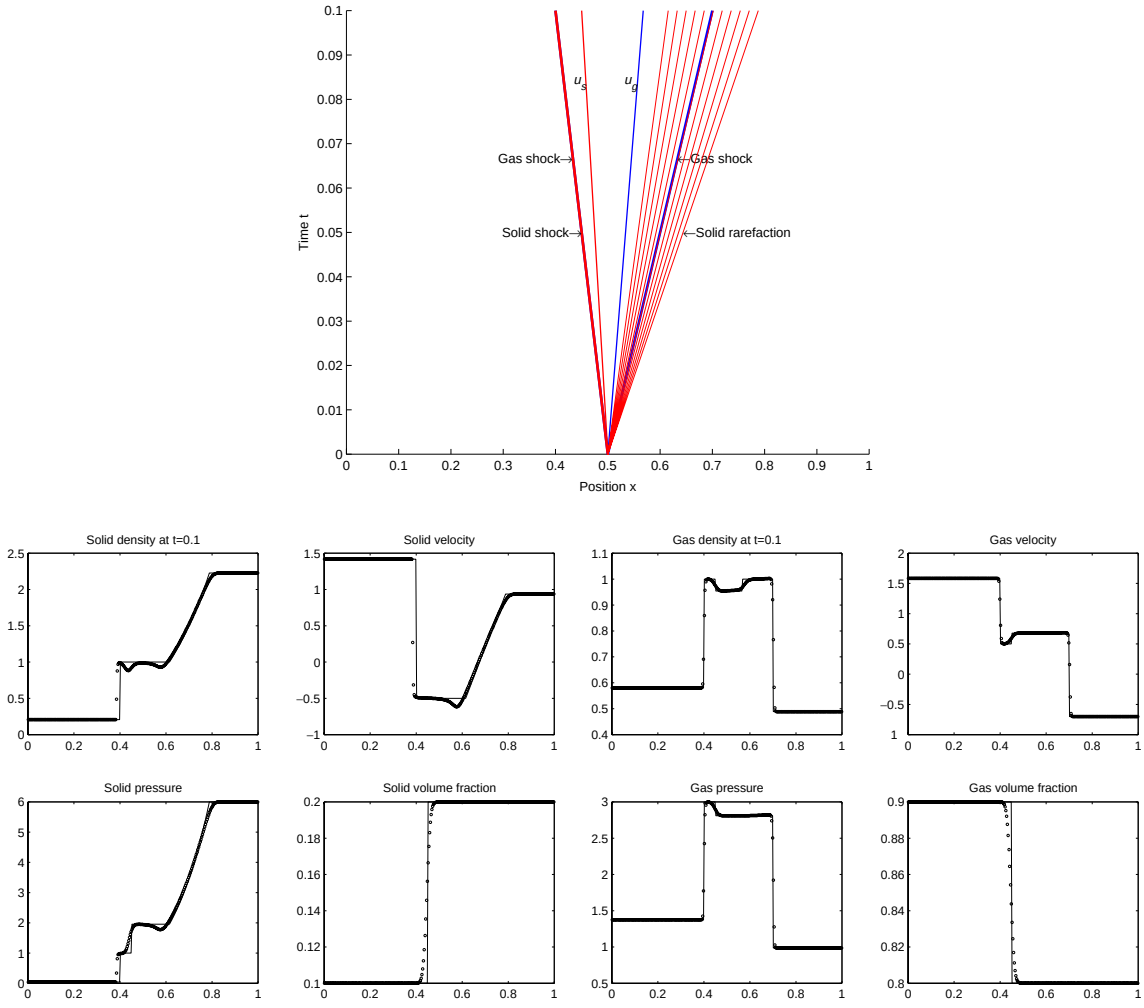

Fig. 8. The Riemann problem for Test 2.

The exact solution to this test consists of a gas rarefaction, approaching the solid contact from the left. In the limit, a parabolic degeneracy occurs, see Section 8.3. The structure of the Riemann problem and the numerical results are shown in Fig. 11.

9.3. Discussion of numerical results

The presented results have a very different quality for the various configurations. When the jump in volume fraction is not too big, the method is quite reliable, see e.g. the results for the Euler equations in the duct in Fig. 6. As expected, the results are also good for Test 3, see Fig. 9.

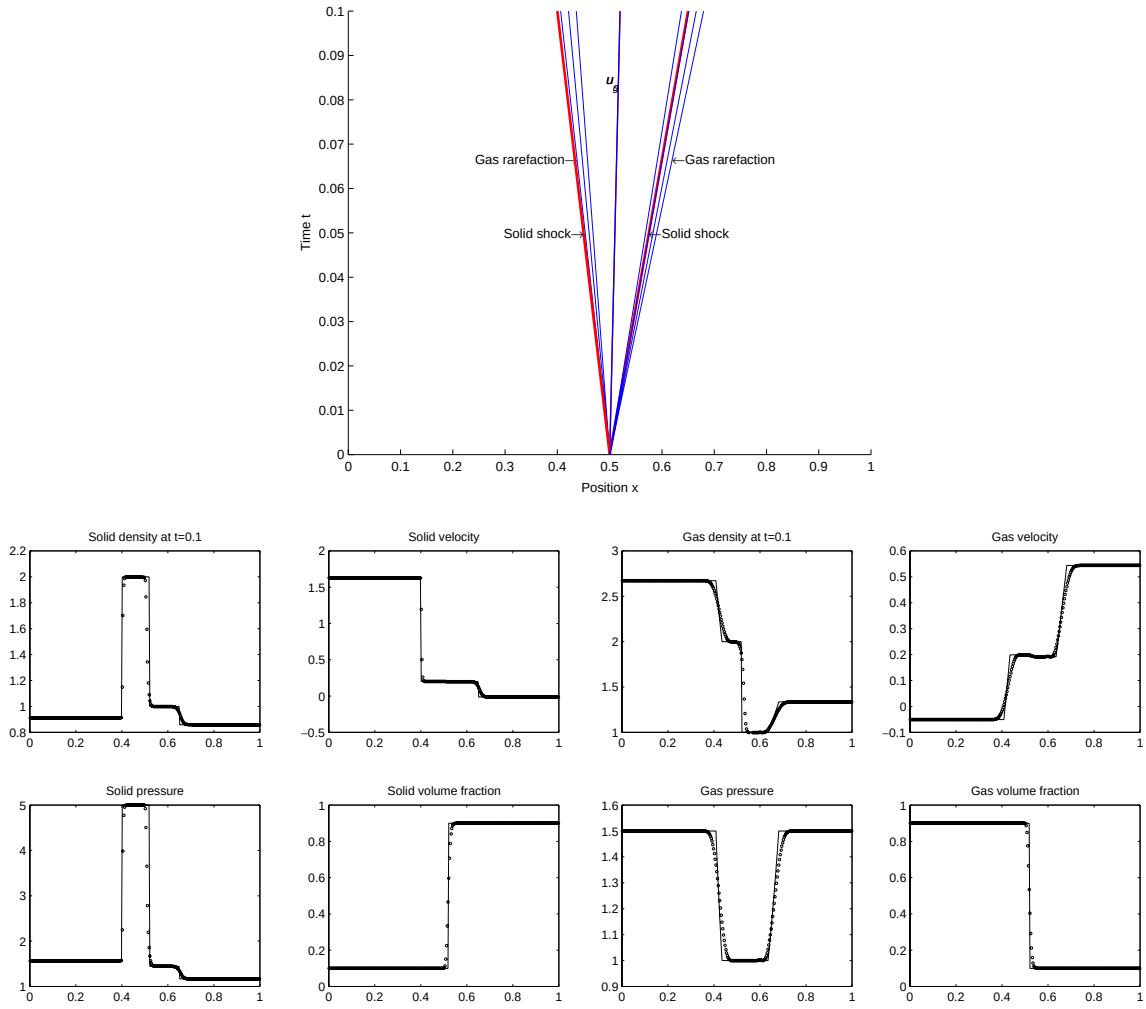

Fig. 9. The Riemann problem for Test 3.

However, it is obvious that for big jumps in volume fraction the VFRoe method gives inadequate results. The numerical solution exhibits oscillations near the solid contact, which do not disappear as the mesh is refined. In the course of time, these oscillations are transported downstream, see e.g. the results for Test 1 in Fig. 7. The results for Test 2 in Fig. 8 show that the waves in different phases affect each other, which should not be the case. Observe the undershoots in solid density and velocity in Fig. 8. The methods behaves unsatisfactory in Test 4, where the gas shock approaches the solid contact. The numerical solution deviates strongly from the exact one, see Fig. 10. The reason for this is clear: The discretization of the non-conservative terms in VFRoe is obtained for the special case of constant

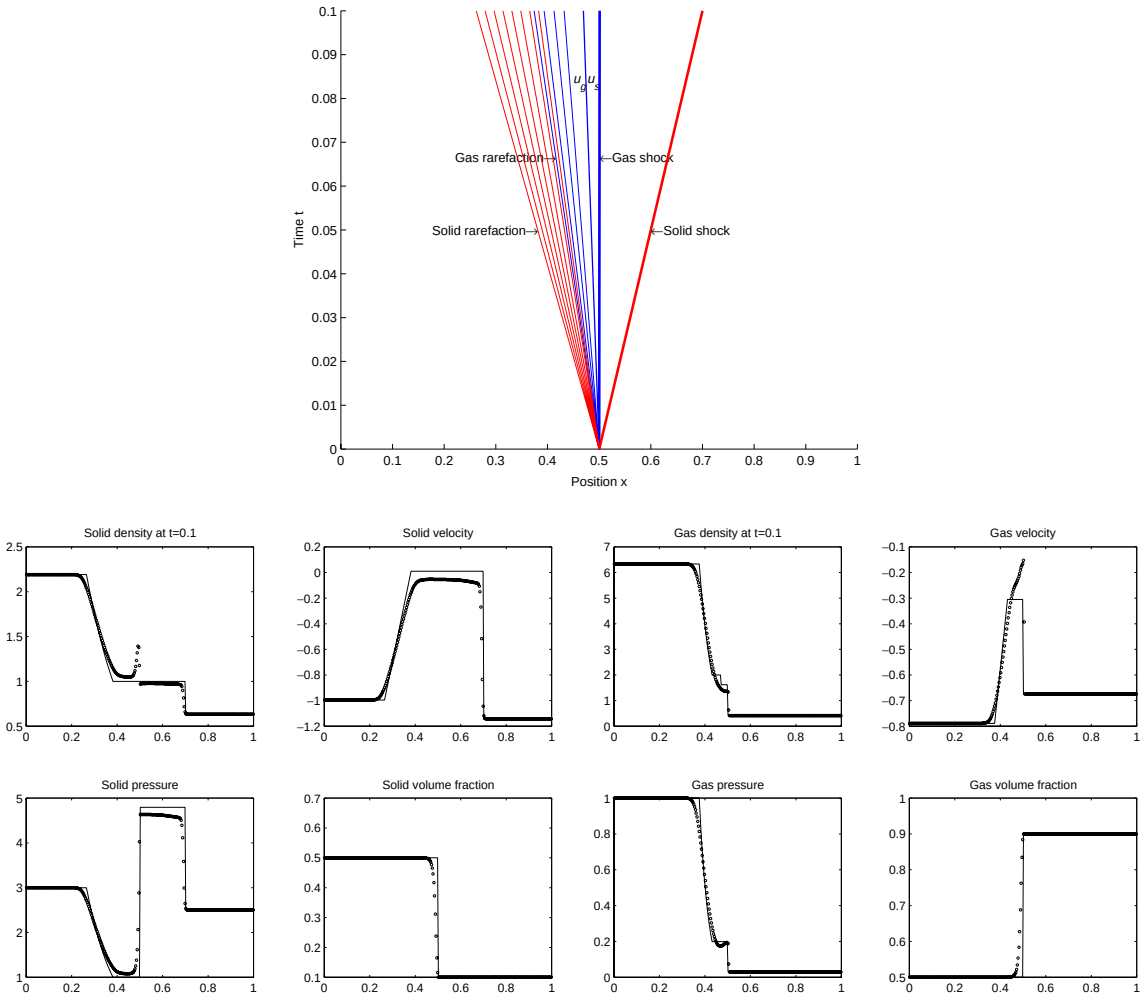

Fig. 10. The Riemann problem for Test 4.

velocity and pressure, see [3] for details. For Test 4, this is of course violated, which leads to wrong numerical results in Fig. 10.

10. Conclusions

The investigation of the non-conservative, non-strictly hyperbolic BN model [5] is difficult from both analytical and numerical points of view. The analytical solution to the Riemann problem for it can be non-unique. For certain initial data, the Riemann solution even does not exist, cf. [4]. On the other hand, it is not clear how to design numerical methods for the BN model. A physically reasonable discretization of non-conservative terms may fail miserably. We believe that this will be also the case for non-conservative models which are similar to the BN model, e.g. the ones introduced in [13,26]. We hope that the test cases of

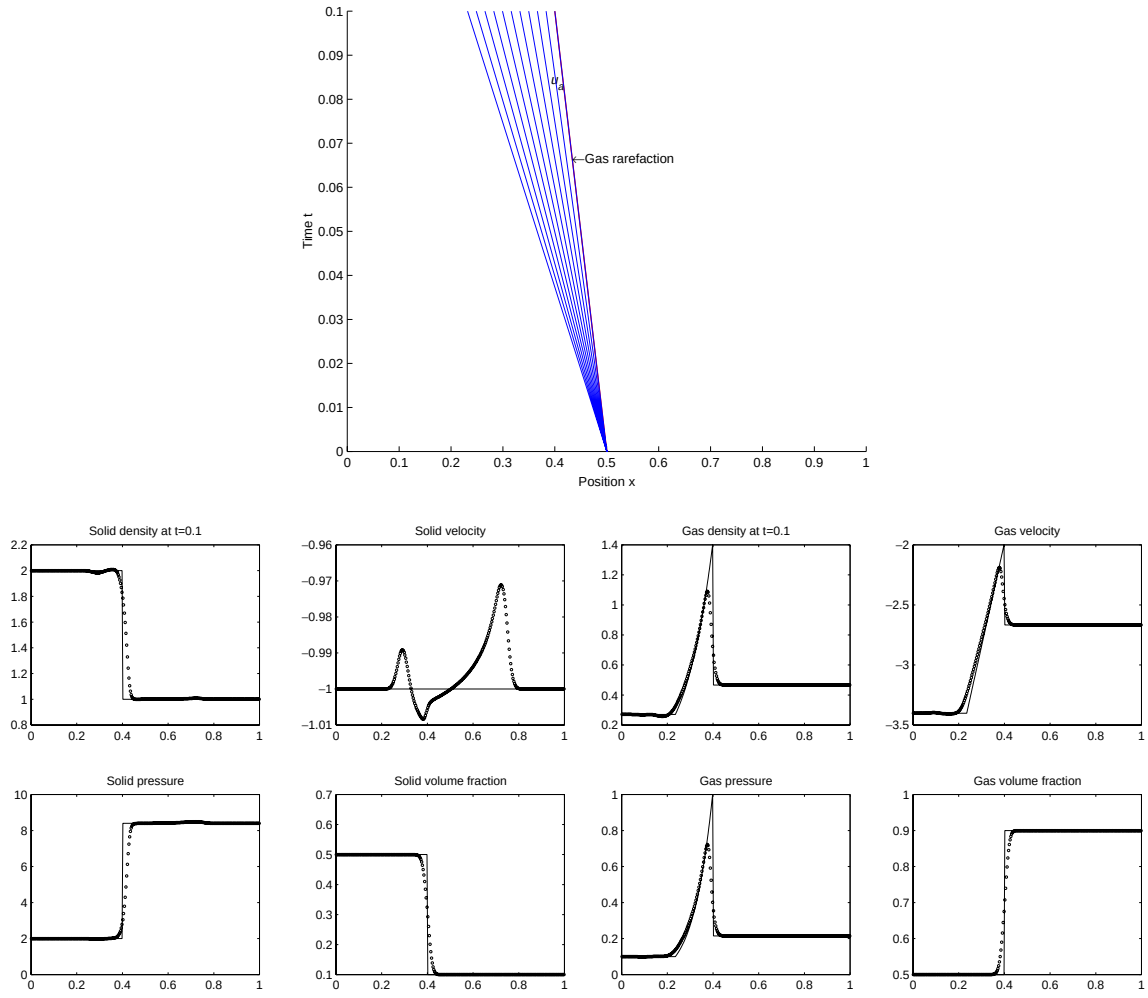

Fig. 11. The Riemann problem for Test 5.

Section 9 will be helpful for constructing of efficient numerical methods for such models. Also, the idea behind the definition of a weak solution of Section 5 may be helpful in designing of approximate Riemann solvers for such models.

References

[1] N. Andrianov, CONSTRUCT: a collection of MATLAB routines for constructing the exact solution to the Riemann problem for the Baer–Nunziato model of two-phase flows. Available from: <http://www-ian.math.uni-magdeburg.de/home/andriano/CONSTRUCT>.

[2] N. Andrianov, Analytical and numerical investigation of two-phase flows, PhD thesis, Universität Magdeburg, 2003. Available from: <http://www-ian.math.uni-magdeburg.de/home/andriano/diser.html>.

[3] N. Andrianov, R. Saurel, G. Warnecke, A simple method for compressible multiphase mixtures and interfaces, Int. J. Numer. Meth. Fluids 41 (2003) 109–131.

[4] N. Andrianov, G. Warnecke, On the solution to the Riemann problem for the compressible duct flow, to appear in SIAM J. Appl. Math.

[5] M.R. Baer, J.W. Nunziato, A two-phase mixture theory for the deflagration-to-detonation transition (DDT) in reactive granular materials, Int. J. Multiphase Flows 12 (1986) 861–889.
[6] J.B. Bdzil, R. Menikoff, S.F. Son, A.K. Kapila, D.S. Stewart, Two-phase modeling of deflagration-to-detonation transition in granular materials: A critical examination of modeling issues, Phys. Fluids 11 (2) (1999) 378–402.
[7] R. Courant, K.O. Friedrichs, Supersonic Flow and Shock Waves, Springer, New York, 1999.
[8] C. Crowe, M. Sommerfeld, Y. Tsuji, Multiphase Flows with Droplets and Particles, CRC Press, Boca Raton, 1998.
[9] G. Dal Maso, P.G. LeFloch, F. Murat, Definition and weak stability of nonconservative products, J. Math. Pures Appl. 74 (1995) 483–548.
[10] D.A. Drew, S.L. Passman, Theory of Multicomponent Fluids, Springer, New York, 1999.
[11] P. Embid, M. Baer, Mathematical analysis of a two-phase continuum mixture theory, Continuum Mech. Thermodyn. 4 (1992) 279–312.
[12] S.A.E.G. Falle, S.S. Komissarov, On the inadmissibility of non-evolutionary shocks, J. Plasma Phys. 65 (2001) 29–58.
[13] S. Gavrilyuk, R. Saurel, Mathematical and numerical modeling of two-phase compressible flows with micro-inertia, J. Comput. Phys. 175 (2002) 326–360.
[14] K.A. Gonthier, J.M. Powers, A high-resolution numerical method for a two-phase model of deflagration-to-detonation transition, J. Comput. Phys. 163 (2000) 376–433.
[15] E. Isaacson, B. Temple, Nonlinear resonance in systems of conservation laws, SIAM J. Appl. Math. 52 (1992) 1260–1278.
[16] E. Isaacson, B. Temple, Convergence of the 2×2 Godunov method for a general resonant nonlinear balance law, SIAM J. Appl. Math. 55 (1995) 625–640.
[17] M. Ishii, Thermo-fluid Dynamic Theory of Two-phase Flow, Eyrolles, Paris, 1975.
[18] A.K. Kapila, S.F. Son, J.B. Bdzil, R. Menikoff, D.S. Stewart, Two-phase modeling of DDT: structure of the velocity-relaxation zone, Phys. Fluids 9 (12) (1997) 3885–3897.
[19] A.K. Kapila, R. Menikoff, J.B. Bdzil, S.F. Son, D.S. Stewart, Two-phase modeling of deflagration-to-detonation transition in granular materials: Reduced equations, Phys. Fluids 13 (10) (2001) 3002–3024.
[20] L.D. Landau, E.M. Lifshitz, Fluid Mechanics, Pergamon Press, Oxford, 1987.
[21] R. Menikoff, B.J. Plohr, The Riemann problem for fluid flow of real materials, Rev. Mod. Phys. 61 (1) (1989) 75–130.
[22] R.I. Nigmatulin, Dynamics of Multiphase Media, Hemisphere, New York, 1991.
[23] J.M. Powers, D.S. Stewart, H. Krier, Theory of two-phase detonation – part I: Modeling, Combust. Flame 80 (1990) 264–279.
[24] V.H. Ransom, Numerical benchmark tests, in: G.F. Hewitt, J.M. Delhaye, N. Zuber (Eds.), Multiphase Science and Technology, 3, Hemisphere, Washington, 1987.
[25] L. Sainsaulieu, Euler system modeling vaporizing sprays, in: Kuhl et al. (Eds.), Dynamics of Heterogeneous Combustion and Reacting Systems. Progr. Astronaut. Aeronaut., 152 (1993).
[26] R. Saurel, R. Abgrall, A multiphase Godunov method for compressible multifluid and multiphase flows, J. Comput. Phys. 150 (1999) 425–467.
[27] R. Saurel, O. LeMetayer, A multiphase model for compressible flows with interfaces, shocks, detonation waves and cavitation, J. Fluid Mech. 431 (2001) 239–271.
[28] J. Smoller, Shock Waves and Reaction–Diffusion Equations, Springer, New York, 1983.
[29] E.F. Toro, Riemann Solvers and Numerical Methods for Fluid Dynamics, Springer, Berlin, 1999.
[30] M.J. Zucrow, J.D. Hoffman, in: Gas Dynamics, vol. 2, Wiley, 1977.